Development of a desktop STM using ballistic electron emission microscopy and spectroscopy to study Ni-SiC Schottky contacts.

Al-Hartomy, Omar A

Development of a Desktop STM using Ballistic Electron Emission Microscopy and Spectroscopy to Study Ni-SiC Schottky Contacts

By

Omar A. Al-Hartomy

University of Wales Swansea

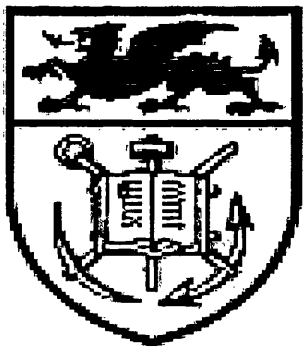

Department of Physics

May 2005

This thesis is submitted to the University of Wales Swansea in candidature for the Degree of Master of Philosophy

ProQuest LLC.
789 East Eisenhower Parkway
P.O. Box 1346
Ann Arbor, MI 48106 – 1346

DECLARATION

This work has not previously been accepted in substance for any degree and is not being concurrently submitted in candidature for any other degree.

Signed .... (candidate)

Date .....Thu..27th..May..2005

STATEMENT 1

This thesis is the result of my own investigations, except otherwise stated. Other sources are acknowledged by footnotes giving explicit references. A bibliography is appended.

Signed ..... . (candidate)

Date .....Thu..27th..May..2005

STATEMENT 2

I hereby give consent for my thesis, if accepted, to be available for photocopying and for inter-library loan, and for the little and summary to be made available to outside organisations.

Signed .... (candidate)

Date .....Thu..27th..May..2005

This thesis is dedicated to my country, my parents, my wife and my sons

ACKNOWLEDGEMENTS

I would like to express my great appreciation and sincere gratitude to my supervisor Dr. Peter Dunstan for his suggestion of the area of my research, his invaluable supervision, his advice, his guidance and his help throughout my studies.

It is a pleasure to express my thanks to Mathew Ackland, Mark Holton, Richard Baylis and Jeffery Kettle for their advice, laboratory assistance, discussions and friendly atmosphere. I would also like to thank the Head of the Department Professor Mike Charlton and the technical support Julian Kivell and Mike Rogers together with other support staff within the department.

I would also like to thank Dr. Owen Guy for his help in preparing the samples and Professor Paul Rees for his help in modelling the BEEM spectra. A special thanks and appreciation to Mathew Ackland for his patient proof reading.

I am very grateful to my parents, my wife and my sons, for their patience, encouragement and support throughout my studies.

Finally, I wish to thank King Abdul Aziz University in Saudi Arabia for providing financial support during my studies at the University of Wales, Swansea.

ABSTRACT

Ballistic electron emission microscopy and spectroscopy (BEEM/BEES) have been employed by developing a basic desktop STM in air in order to study Ni-SiC samples. The electronic properties of Ni contacts to SiC are highly dependent on their manufacturing process and this study generated suitably thin contacts for BEEM measurements that were Schottky in nature and made under UHV evaporation conditions. The sample also required an Ohmic contact to allow the detection of the BEEM current and these were formed using an Edwards evaporator. BEEM is a three terminal measurement based upon the generation of pico amp currents and as a result amplifier circuits with I/V conversion were used to amplify the BEEM current to give a voltage in the range of $\pm 10\,V$ for input into an auxiliary channel of the basic STM control unit. Also, a sample holder ($110\,mm \times 210\,mm$) was modified which allowed a 3rd contact to the sample within the usual STM set-up.

During this work, simultaneous STM and BEEM images have been recorded at various tunnelling currents and bias voltages. These images show distinct differences and the interface behaviour appears modified by varying electrical properties between the Ni and SiC which are resolved spatially on the nanoscale within the BEEM image. Furthermore, measurements were made to determine the Schottky barrier height values using BEES in different locations by observing the ballistic current as a function of voltage. It was found that the Schottky barrier varied between 1.48 eV to 2.35 eV depending on the region or features analysed. The interaction at room temperature between Ni and SiC is discussed in light of these measurements and compared to current literature to resolve the origin of the observed Schottky barrier height variations.

CONTENTS

Chapter 1

Introduction

1.1 General introduction

Metal semiconductor interfaces have generated wide interest for more than a century[1]. However, current trends develop new materials and nano-dimensional system requires high resolution characterisation in order to improve device reliability and performance. Thus there is an increasing demand for nano-scale probes of electronic properties for semiconductor devices, such as metal-semiconductor junctions. The macroscopic electronic structure of Schottky interfaces can be studied by examining the electrical behaviour of the junction that is represented by the I-V characteristic and ideality factor[2,3]. There are a large number of technological applications of a metal semiconductor junction, such as Schottky diodes, metal semiconductor field-effect transistors, hot electron transistors and high speed devices[2]. Many different experimental techniques have been developed to investigate the electronic structure and electrical behaviour of metal semiconductor interface. In this work, the hot electron

transport between a semiconductor surface covered with thin metal is investigated using the ballistic electron emission microscopy (BEEM) technique.

One technique which has been used with great accomplishment to study semiconductors with atomic resolution is scanning tunnelling microscopy (STM). Since the first atomic resolution images were obtained by Binning and Rohrer[4] in 1982, STM has become one of the most powerful surface analysis techniques available to investigate the structure and electronic properties of sample surfaces[5]. Scanning tunnelling spectroscopy (STS) is a complementary technique used with STM to study the local electronic properties of a sample, such as the Fermi energy and local band- structure properties.

Ballistic electron emission microscopy (BEEM) is a different approach used to investigate metal-semiconductor interfaces using a STM technique. BEEM was invented by Kaiser and Bell[6] in 1988 and is used to investigate the electrical properties of buried interfaces. It also has the capability to obtain images with nano-scale resolution of buried structures and enables the characterisation of junctions between metals and n-type semiconductor. Moreover, ballistic electron emission spectroscopy (BEES) is also a powerful tool to characterise and record information at a specific location on the sample. BEES has been used widely with BEEM to determine the Schottky barrier heights of metal-semiconductor junctions.

The work presented here aimed to use BEEM/BEES to study a metal-semiconductor sample in air using a desktop STM. The samples which have been used during this work are Schottky Ni-(4H)SiC samples and they were made using different equipment to make the samples suitable for the BEEM investigation. Contacts to SiC are important for development of high temperature and power electronics and thus fully understanding contact properties is

crucial. BEEM and BEES contribute greatly and is one of the goals of this work. In addition, the system for BEEM was designed to be compatible with a desktop STM along with the three contact measurements. BEES was utilized to allow the current–voltage characteristics of a localised point at the interface to be investigated from the surface.

1.2 Thesis outline

In chapter 2 a brief history of metal-semiconductor contact theory is presented, including the basic theory of rectifying metal-semiconductor contacts (Schottky-Mott theory). An overview of current transport through the metal-semiconductor interface and the I-V technique are included along with basic information SiC. In chapter 3 is discussed the basic principle and theory on which STM and STS are found. The quantum mechanical tunnelling phenomena used by STM are introduced, followed by the theory of imaging mode. An example of an STM image is given together with a brief outline about STS. In chapter 4 a description of the BEEM technique is provided, followed by a survey of BEES and BEEM literature. The main apparatus developed for BEEM and BEES, which has been used throughout this work, is described in chapter 5, including instrumentation, development of the system and sample preparation. The development of the electronics circuitry and final set-up are provided. Testing the STM and BEEM technique are presented and the important results of Ni/SiC contacts are reported in Chapter 6. In addition, Schottky barrier height values are extracted from BEEM images and spectra in this chapter. Finally, conclusions and future work are presented in chapter 7.

1.3 References

[1] F. Braun, Pogg. Ann. **153**,556 (1874).

[2] S.M. Sze ,physics of semiconductor device ,(Wiley,NY,1969).

[3] E.H. Rhoderick , Metal –Semiconductor Contacts (Thomason Ltd , Scotland 1978).

[4] G.Binning, H.Rohrer, Ch.Gerber, and E.Weibel, Phys. Rev. Lett, **49**, 57(1982).

[5] J.Tersoff ,N.D. Lang ,"Methods od Experimental Physics : Scanning Tunnelling Microscopy"Chapter1,**1-3**,Edit.J.A. Stroscio and W.J. Kaiser , Academic Press (1993).

[6] W.J. Kaiser and L.D. Bell, Phys. Rev. Lett. **60**, 1406 (1988).

Chapter 2

Metal-Semiconductor Contacts

2.1 Introduction

Metal to semiconductor contacts are of great importance since they are present in every semiconductor device. Two types of contacts exist, and the electronic properties of metal-semiconductor contacts, i.e. the current-voltage (I-V) characterisation, classify the formation of the contact. Electrical contact to semiconductors is facilitated by Ohmic metal-semiconductor contacts that exhibit linear current-voltage (I-V) characteristics and present low contact resistance to current transport in both directions (i.e. forward and reverse bias's). The other type of contact possesses a potential barrier at the metal-semiconductor interface, which exhibits rectifying nature; i.e. it only allows current to flow in one direction. Such contacts are voltage dependent and are essential in the formation of diodes; they are known as Schottky contacts. This study utilises the STM- based BEEM technique to characterise the nano-scale structure of Schottky contacts, which are theoretically discussed within this chapter.

2.2 Silicon Carbide

Jöns Jacob Berzelius was the first man to investigate SiC in 1826[1], SiC properties were not known precisely at that time but with demands for high power electronic devices interest in SiC has increased. Silicon carbide is currently under intensive investigation as an enabling material for a variety of new semiconductor devices specifically in areas where silicon devices cannot effectively compete. It has good mechanical and electrical properties, such as high thermal conductivity, high current density and wide band gap[2] (~ 2.4 - 3 e*V*) depending on its polytype, which make it suitable in the application of high voltage and power transmission. The critical field strength is ten times larger than Si and its band gap is about three times larger than that of Si[2] at 3.2 *eV*. 4H-SiC Schottky diodes contain many attractive features, such as, high temperature, capability under reverse bias, fast switching speed and a significant reduction of switching losses[3].

The success of SiC lies in its capability to form stable metal contacts of both Schottky and Ohmic character. However, the study of metal-SiC contacts requires optimisation in order to produce more stable devices. New experimental and theoretical evaluations are required to investigate the basic properties of the Schottky SiC contact, such as using the BEEM technique developed here using a desktop, ambient STM system.

2.3 Schottky contact formation

Consider the energy band diagrams of the separate metal and semiconductor, before contact formation, as shown in figure 2.1 which uses the same vacuum level. The Fermi energy levels of the metal and semiconductor are indicated as E_F^m and E_F^s respectively, and

are dependant on the doping in the case of the semiconductor (in this case example, n-type). The work function of the metal is ϕ_m, and the work function of semiconductor is ϕ_s, which represent the energy separation between the Fermi level and the vacuum level (in electron-volts,eV) before contact is made, in the example the case of $\phi_m \rangle \phi_s$ is considered. The energy difference between the vacuum level and the bottom of the semiconductor conduction band is referred to as the electron affinity and is denoted by χ_s. Hence the minimum energy required to release an electron from the semiconductor is such that $\phi_s = \chi_s + \xi$ where ξ is known as the chemical potential and determined by the position of the Fermi level relative to the conduction band, as shown in figure 2.1.

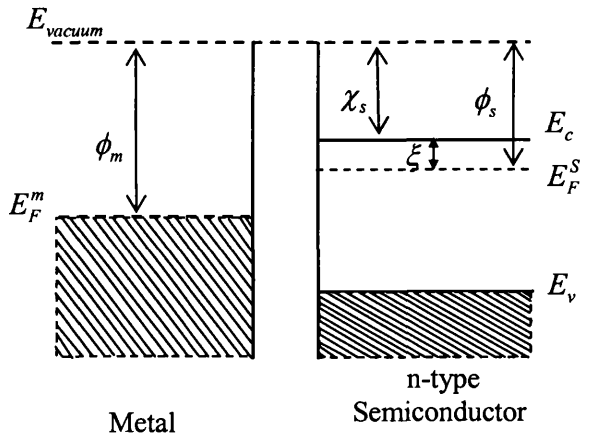

Figure 2.1: Energy band diagram of the isolated metal and semiconductor relative to the vacuum level.

When a metal and a n-type semiconductor are brought into intimate contact, electrons from the semiconductor will move into the metal resulting in equilibrium of the Fermi levels of the metal and semiconductor across the interface. As the electrons leave the semiconductor, a positive charge, caused by the static uncompensated donor atoms remains,

creating a positive region at the boundary of the semiconductor, which is called the depletion region. A dipole field is established between the positively charged depletion region of the semiconductor and the thin layer of negative charge at the surface of metal, known as the electron accumulation region, this eventually opposses further charge diffusion and an equilibrium at the interface is established. The alignment of the Fermi levels across the interface and charge depletion within the semiconductor leads to band-bending of the semiconductor energy bonds at the inteface, the the formation of the Schottky barrier, ϕ_b, at the interface, as seen in figure 2.2.

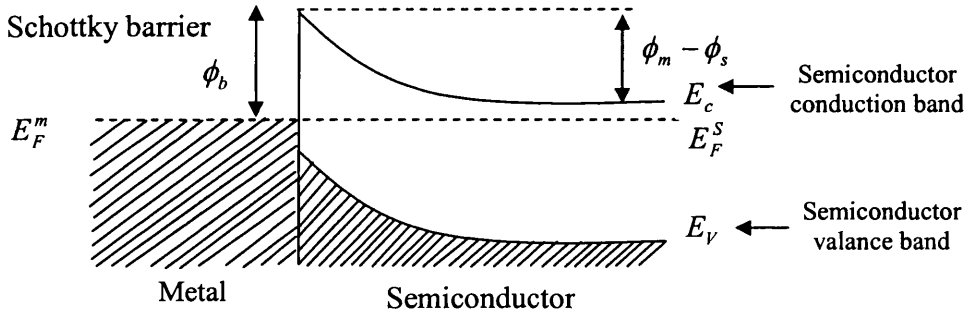

Figure 2.2: Schottky barrier between a metal and an n-type semiconductor.

This model of the metal-semiconductor interface is based upon the depletion region approximation. According to this situation, the negative charge on the metal surface consists of extra conduction electrons and these electrons are contained within the Thomas-Fermi screening distance[5] (≈ 0.5 Å), as shown in figure 2.3.

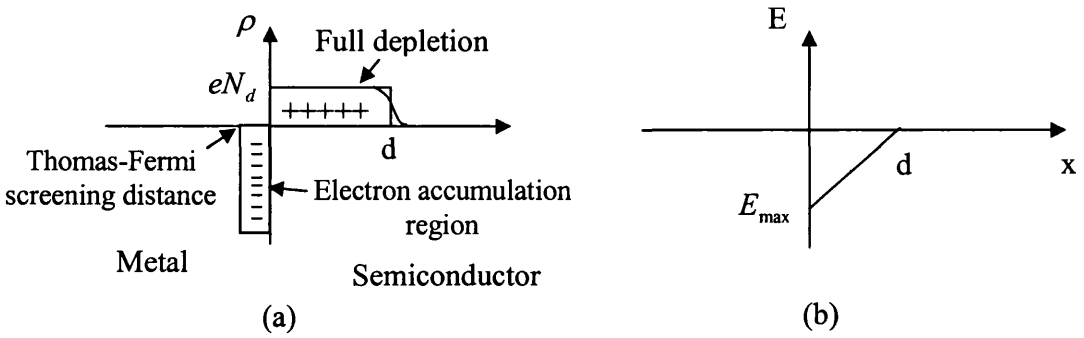

Figure 2.3: (a) Charge density and (b) electric field in the full depletion region.

2.3.1 Schottky-Mott theory

The Schottky-Mott theory is rather simplistic in the sense that it assumes the flat-band condition for the n-type semiconductor, i.e. there is no electric field in the semiconductor[4]. As a result, this implies that the semiconductor terminates at the surface without distortion of the electronic energy levels and there are no electronic states that exist at the surface. The barrier energy ϕ_b is defined as the energy difference between the Fermi level in the metal and the bottom of the conduction band in the n-type semiconductor at the interface and can be givin by Schottky-Mott limit as follows:

$$\phi_b = \phi_m - \chi_s \qquad (2.1)$$

Where, ϕ_b is the contact barrier height, ϕ_m the work function of metal and χ_s the electron affinity of the semiconductor.

The magnitude of the barrier between the metal and semiconductor dictates the extent of the depletion region. Figure 2.3(b) shows the relationship between field and depletion region from $x = 0$ to $x = d$. The depletion layer width is intrinsically linked to the

potential within the semiconductor. The charge density in the depletion region is due to the ionized donor as shown in figure 2.3.

2.3.2 The Bardeen model - surface and interface states

In this model, the Schottky barrier height, ϕ_b, should depend on the metal work function, ϕ_m , as in the Mott theory eq. (2.1). However, there are surface states localised at the surface of the semiconductor[4], in a thin insulating layer located between the metal and the semiconductor possessing a continuous distribution of the surface states, as illustrated in figure 2.4.

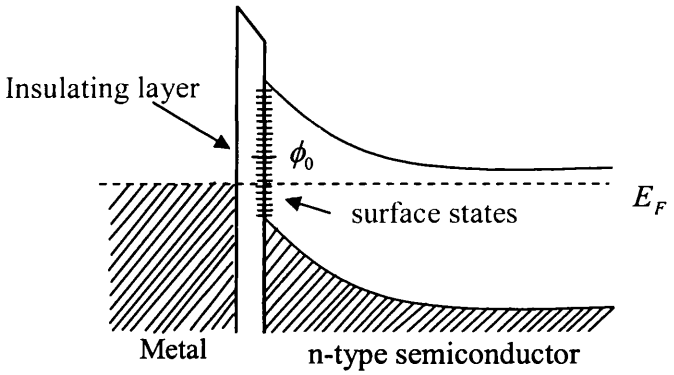

Figure 2.4: Metal contact to n-type semiconductor with surface states presented[5].

The energy position of the surface states relative to the Fermi level at the surface determines their occupancies. When the energy level is measured relative to the valance band, the surface states are characterised by a neutral level, ϕ_0, to which the suface states are filled when the surface is neutral.

The negative charge ϕ_m on the surface of metal has to be equal to the positive donor ions as the junction is electrically neutral, in the absence of surface states. If the neutral level ϕ_0 is above the Fermi level, the suface states contain a positive charge as shown in figure 2.4. As a result, the depletion region is reduced. On the other hand, the depletion region and the Schottky barrier are increased when the neutral ϕ_0 is below the Fermi level and the surface states are negatively charged. If the density of surface states is very large, the Fermi level at the surface of the semiconductor will be at ϕ_0. If an interfacial layer exsits and the surface state density is large, the potential difference $\phi_m - \phi_s$ will cross the interfacial layer since the charge in the surface states will assist the necessary potentail differernce. The metal and semiconductor Fermi levels are the same at the inteface, and the barrier height can be obtained by

$$\phi_b = E_g - \phi_o \tag{2.2}$$

This equation is called Bardeen limit[5], where the barrier is independent of the work function of metal ϕ_m and the Fermi level is pinned or stabilized by the suface states to the neutral level energy above the valance band.

2.4 Ohmic contacts

A metal-semiconductor contact that has a negligible contact resistance relative to the bulk resistance of the semiconductor and a linear I-V characteristic at both forward and reverse bias is known as an Ohmic contact. Ohmic contacts are necessary in all semiconductor devices in order to connect the semiconductor to external circuitry[6].

An Ohmic contact may be manufactured between a metal and semiconductor by introducing a very highly doped region at the semiconductor contact surface in order to produce a very narrow barrier with a thin depletion region. The barrier produced is so thin as to appear transparrent to electron conductors, thus resulting in a linear I-V curve. Ni-SiC Ohmic contacts are thought to be produced in this way via an annealling method. The as-deposited Ni-SiC contact is naturally Schottky in nature, however by annealling to 1000 ^{0}C for 10 minutes in high vacuum, an eutectic liquid is formed at the interface in which the metal diffuses into the semiconductor region. Thus resulting in a suitably thin interface barrier and linear I-V behaviour[4,5]. An Ohmic contact can also be formed via other methods. The Schottky-Mott theory predicts a negligible barrier if the semiconductor electron affinity matches the metal work function. Also by increasing interface states a reduced resolution is possible due to the recombination of charges in space charge region.

2.5 Current transport

The movement of electrons is mainly due to their vast number. For the metal-semiconductor under forward bias, current flows by thermionic emission and field emission. In thermionic emission, the transport of electrons is from the semiconductor over the potential barrier into the metal, as seen in figure 2.5(a). In field emission, electrons tunnel quantum mechanically through the whole barrier, as shown in figure 2.5(b).

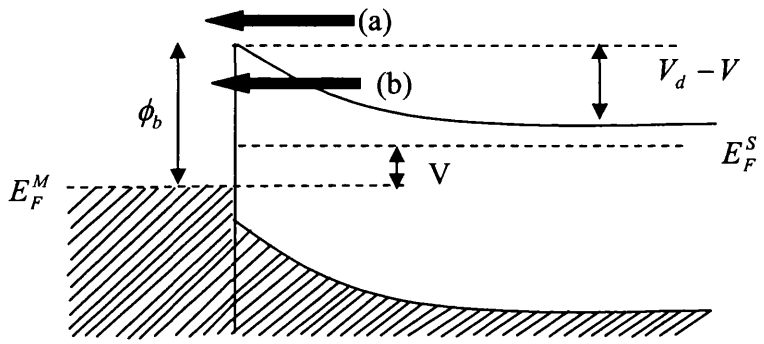

Figure 2.5: The basic transport processes under applied forward bias voltage.

2.5.1 Thermionic emission

The transport of electrons over the barrier is called thermionic emission[7]. In an n-type semiconductor the barrier height should be larger than the thermal equilibrium ($e\phi_b \rangle\rangle k_B T$). The thermionic transport under forward bias allows electrons to travel from the semiconductor to the metal. However, these electrons should have kinetic energy greater than $V_d - V$ (see figure 2.5) to overcome the barrier into the metal, and the drift and diffusion that occur as a result of collisions in depletion region[4]. The distribution of energy when the electrons flow over the barrier into the metal will be in equilibrium with their population in the semiconductor and they are distributed according to Maxwell's distribution. The current density I for an applied bias V is then[6]

$$I = A^* T^2 \exp\left(\frac{-e\phi_b}{k_B T}\right)\left[\exp(eV/k_B T) - 1\right] \tag{2.3}$$

The parameter A^*, is known as Richardson's constant for thermionic emission and is giving by

$$A^* = \frac{4\pi e m_e^* k_B^2}{h^3} \tag{2.4}$$

Here m_e^* is the effective mass of the majority of electrons, T is temperature, k_B is Boltzmann's constant and h is Plank's constant. When $m_e^* = m_0$ for the free electron mass, $A^* = 120\,A/cm^2K^2$. Note the values of A^* and m_e^* are dependent upon the band structure of the semiconductor. The current-voltage (I-V) characterisation of Schottky diodes can be obtained by equation (2.3) by assuming that the barrier height is independent of the applied bias. The actual situation is more complicated as the applied Schottky barrier $\phi_b^{applied}$ depends on the electric field in the semiconductor which is affected by the applied bias V. A Taylor series[8] expansion highlight the dependence of the applied Schottky barrier $\phi_b^{applied}$ on V by equation

$$\phi_b^{applied} = \phi_b + \beta V \tag{2.5}$$

Where ϕ_b is the barrier energy at zero bias and β is a constant. As the equation (2.5) is substituted into equation (2.3) that gives

$$I = A^*T^2 \exp\left(\frac{-e\phi_b}{k_BT}\right)\exp(eV/nk_BT) \tag{2.6}$$

It is expressed as follows

$$I = I_0 \exp(eV/nk_BT) \tag{2.7}$$

And I_0 is defined as

$$I_0 = A^*T^2 \exp\left(\frac{-e\phi_b}{k_BT}\right) \tag{2.8}$$

$$n = (1-\beta)^{-1} \tag{2.9}$$

The parameter n is called the ideality factor of the Schottky barrier. When the value of n=1.0, the current-voltage (I-V) characteristic of junction between the metal and the semiconductor is that an ideal Schottky diode. A Schottky contact possessing non-uniform barrier properties is represented by an ideality factor which is greater than one (i.e. $n \rangle 1$).

2.5.2 Field emission

Quantum mechanical tunnelling across the metal-semiconductor interface is the kind of current transport which dominates the characteristics of an ohmic junction. An ohmic contact is characterised by a linear I-V curve and non-rectifying properties. For high doping levels, the barrier is sufficiently thin for quantum mechanical tunnelling of electrons through the barrier to occur. The electrons are emitted directly from states at Fermi level in the semicoductor to occupy all available energy levels in the metal, and this is known as field emission[9,10].

2.6 I-V Technique

In recent years, several different macroscopic techniques such as capacitance-voltage(C-V)[5,11], current-voltage (I-V)[5], x-ray photoelectron spectroscopy (XPS), and photoresponse or (photocurrent)[12] have been used to investigate the properties of Schottky contacts[13,14]. Current-voltage (I-V) relationships investigate the electrical characteristics of Schottky rectifiers such as the barrier height, ϕ_b, and ideality factor[5], n. The measurement of current –versus- voltage curves (I-V) is one of the most important and widely applied technique for characterising such contacts. The current is measured as a function of the

applied voltage which is performed at a constant temperature and under dark conditions, and is measured inside a faraday cage to eliminate the noise influence of external sources. The Schottky barrier height can then be calculated from the I-V curve, as the I-V measurement data can also be fitted according to the equation (2.7) in the form of a ln(I) versus V

$$\ln(I) = \frac{e}{nk_BT}V + \ln(I_0) \qquad (2.10)$$

A straight line can be plotted from equation (2.10) of ln(I) vesus V and then the value of I_0 will be obtained and substituted into equation (2.8) to calculate the Schottky barrier value

$$\phi_b = -(k_BT/e).\ln(I_0/A^*T^2) \qquad (2.11)$$

The gradient of the straight line is given by e/nk_BT, and is used to evaluate the ideality factor n. The Schottky barrier values for an n-type semiconductor are evaluated with an accuracy of $\pm 10.0\,\%$[4].

2.7 Summary

This chapter has briefly discussed the important background of aspects to the formation of Schottky contacts and current transport mechanisms, as well as providing some brief background to SiC. Important aspects of current measurements are outlined in which will be referred to later in the thesis. For further details the reader is directed to the reference list, particular Rhoderick and Williams[5].

2.8 References

[1] J.J. Berzelius, Ann. Phys., Lpz., **1**, 169, (1824).

[2] M. Sochacki, J. Szmidt, A. Werbowy, J. Wide Band-gap Matt. **9** (4),307 (2002).

[3] R. Rupp, M. Treu, A. Mauder, E. Grieble,W. Werner,W. Bartsch and D. Stephani,Mater. Sci. Forum, **338**,1167 (2000).

[4] C. W. Wilmsen, Physics and Chemistry of III-V Compound Semiconductor Interfaces,(Plenum,NY,1985).

[5] E.H. Rhoderick and R.H Williams, Metal –Semiconductor Contacts (Oxford University Press, 2nd Edition, 1988).

[6] S.M. Sze ,physics of semiconductor device ,(Wiley,NY,1969).

[7] H. A. Bethe, Theory of the boundary Layer of Crystal Rectifiers, MIT Radiation Lab. Report **43-12** (1942).

[8] V.Heine, Phys. Rev. A. **138**, 1689 (1965).

[9] F. A. Padovani, R. Stratton, Solid-State Electron. **9**, 695 (1966).

[10] C.R. Crowell, V.L. Rideout, Solid-State Electron. **12**, 89 (1969).

[11] Y.P. Song, R.L. Van Meirhaeghe, W.H. Laflere, F. Cardon, Solid-state Electron.,**29**, 633 (1986).

[12] T. Dell'Orta, J.Almeida, C. Coluzza, A. Baldereschi, G. Margaritondo, M, Cantile, S. Yildirim, L. Sorba, and A. Franciosi, Appl. Phys. Lett. **64** (16), 2111 (1994).

[13] L. M. Porter and R.F. Davis, Mater.Sci. Eng. B **34**,83(1995).

[14] J.R. Waldrop, R.W. Grant, Y. C. Wang and R.F. Davis, J. Appl. Phys. **72**, 4757(1992).

Chapter 3

Scanning Tunnelling Microscopy (STM)

3.1 Introduction

In the early 1980's two IBM scientists, Binning and Rohrer[1] developed a new technique for studying surface structure called scanning tunnelling microscopy (STM). Their accomplishment, which won them a Nobel Prize in 1986, utilized the every day basics of quantum mechanics and produced a revolutionary method for determining surface structure on an atomic scale, and which continuous to have a great impact on the study of surface structures. It is used to study metals and conducting or semiconducting surfaces and in recent times can provide nano-electronic information. STM has also opened up many new areas of science and engineering at the atomic and molecular level, in fact the development of STM has proven to be an invaluable and unique tool for the determination of both structural and electronic properties of surfaces.

3.2 Basic principle of STM techniques

3.2.1 Quantum tunnelling

The basic principle of STM is based on the quantum mechanical tunnelling effect which explains the idea of an electron passing from one metal across a potential barrier to another. When two electrically conducting materials are brought into close proximity with each other, under the application of an applied bias and separated by a potential barrier which is narrow enough to allow an overlap of the decaying wave functions, electrons will be able to tunnel through the potential barrier[2]. This results in a small current flow between the two conductors due to tunnelling, which in the case of STM are the tip and the sample. The tunnelling current I is extremely sensitive to the distance between the tip and the sample. The current decays exponentially with barrier width[3] (tip-sample distance), as defined by equation 3.1.

$$I \alpha e^{-2kZ} \tag{3.1}$$

Here the tunnel current I, depends exponentially on the wave vector k, which is a function of energy, and the tip-sample separation Z. The tunnelling process between a metallic tip and an n-type semiconductor sample across a vacuum barrier is illustrated in figure 3.1.

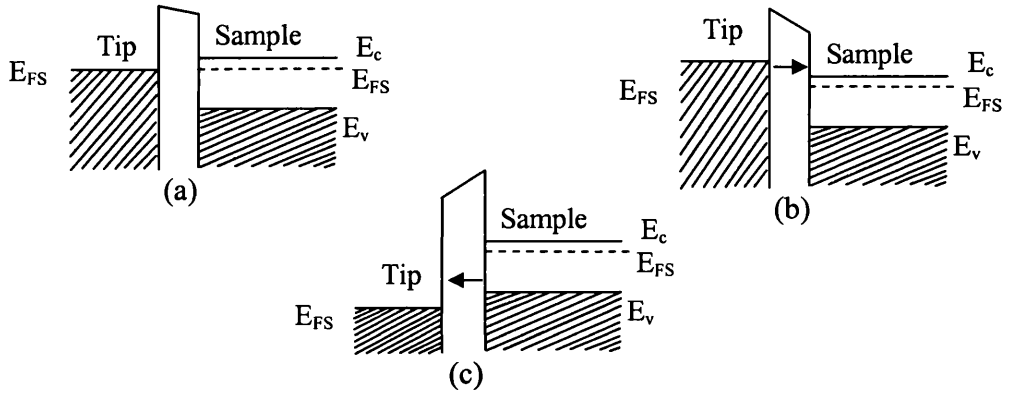

Figure 3.1: Schematic illustrating the tunnelling process between the STM tip and a semiconductor (n-type) sample, when; (a) in equilibrium unbiased, (b) sample biased positively, and (c) sample biased negatively.

In figure 3.1(a), the tip and the semiconductor sample are brought close together. The Fermi level of the tip and the sample are in equilibrium as both tip and sample are at the same zero bias (earth). In figure 3.1(b), when a positive bias voltage is applied to the sample, the energy levels of the sample are shifted to a lower energy state and electrons tunnel from occupied states of the tip into unoccupied states within the conduction band (E_c) of the sample. However, when a negative bias voltage is applied to the sample as shown in figure 3.1(c), the energy levels of the sample are increased in energy and electrons tunnel from occupied states of the sample into the unoccupied states of the tip. Thus the STM can be configured to operate with electrons tunnelling into or out of the sample. When performing ballistic electron emission microscopy imaging, BEEM, the sample is biased positively and electrons tunnel from the tip into the sample, as discussed fully in chapter 4.

3.2.2 Principle of operation

The basic idea of STM is based on the quantum tunnelling phenomenon[2]. A sharp metallic tip, which ideally possesses a single atom at its apex, is brought into close proximity of a few angstroms (Å) with a conductive (or semiconducting) sample surface. By applying a voltage between the tip and the sample, electrons can tunnel quantum mechanically through the vacuum barrier separating the two, and a tunnel current is established flowing from the sample to the tip or from the tip to the sample dependent upon the applied bias as discussed above. Due to the exponential dependence of the tunnel current on the barrier width (equation 3.1), the magnitude of the tunnelling current is highly sensitive to the width of the gap between the tip and the sample.

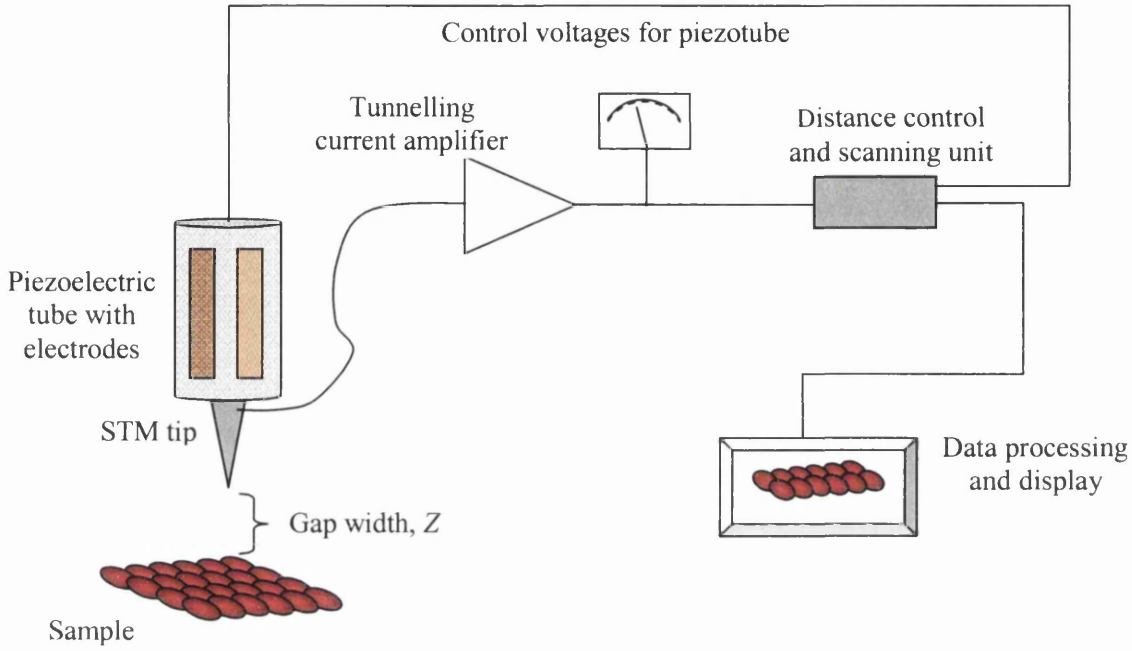

Figure 3.2: Schematic illustrating the operating principle of STM.

The tip is positioned on piezoelectric drivers in order to control the gap width and precisely position the probe to facilitate raster scanning, and pixel image acquisition. The piezoelectric drivers are controlled by the application of an electric field and allow accurate movements on the atomic scale. The feedback loop maintains the tunnel current at fixed value when the tip is scanned across the sample surface. During the scan the voltage applied to the piezoelectric driver which is responsible for the vertical movement, is recorded and is an envoy of the sample topography. Figure 3.2 illustrates the operating principle of the STM.

The tip has to be connected to (x, y, z) as illustrated in figure 3.3(a) which allows for an adjustment of the position of the tip. The adjustment of the tip can be achieved with a high resolution of scanning over the atomic surface, as well as this adjustment depends on the distance between the surface and the sharp head of the tip as shown in figure 3.3(b). The direction of the current flow is determined by the polarity of the bias.

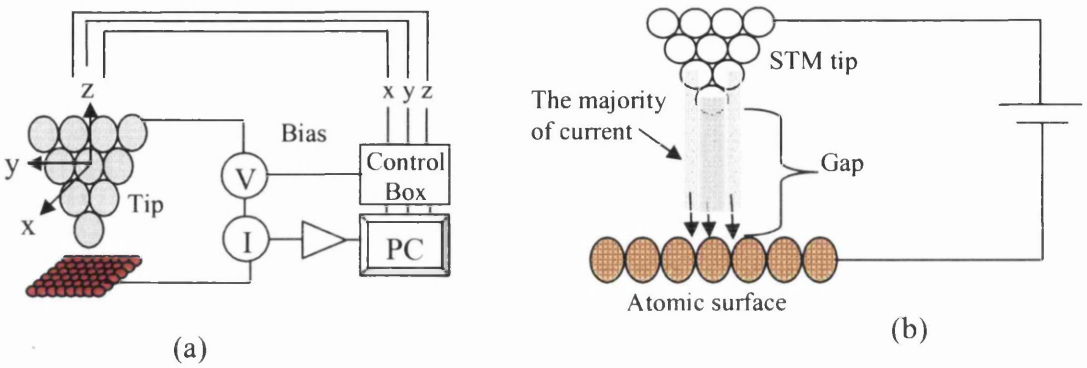

Figure 3.3: (a) Windsor Scientific Ltd nanosurf system, and (b) tunnelling distribution.

3.3 Imaging modes

There are two basic STM modes of operation; these are constant current mode[1] and constant height mode[4], as shown in figure 3.4. These modes are facilitated by the setting the proportional, *P*, and integral, *I*, parameters of the feedback circuit.

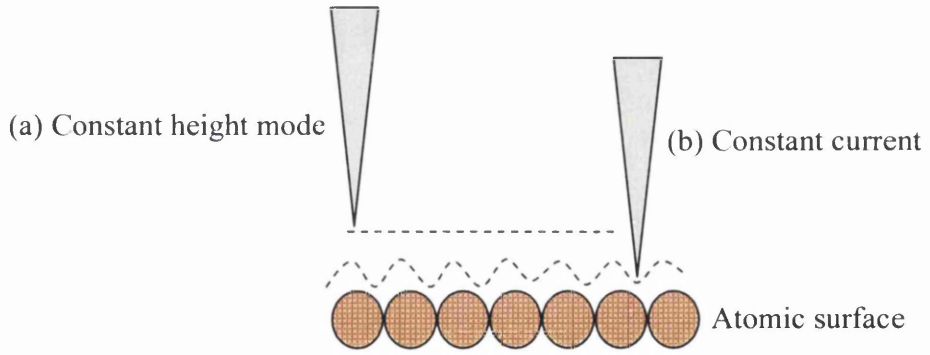

Figure 3.4: STM operating modes, showing (a) constant height mode where the STM tip is rastered at a fixed height and the varying tunnel current is monitored, and (b) constant current mode, where the tunnel current is maintained and the variation in probe height is recorded.

3.3.1 Constant current mode

In constant current mode a feedback loop system adjusts the tip height via a piezoelectric driver in order to maintain the constant tunnel current. A topographical image can be obtained when the tip is raster scanned across the sample surface. The voltage is applied to the piezoelectric driver in order to maintain the constant current. This constant current mode tends to be used for the surfaces which are not atomically flat, and requires careful setting of the finite response time of the feedback loop.

3.3.2 Constant height mode

In constant height mode the feedback system is slowed or disabled and the tip can be scanned rapidly at constant height over the sample surface. The topographic information of the surface can be inferred from the variations in the tunnelling current which are recorded as a function of position. The constant height mode presents a faster scan rate since it is not limited by the response time of the feedback loop. However, the constant height mode is only suitable for atomically flat surfaces, otherwise the tip might crash if the surface is rough.

3.4 Examples of STM images

The interpretation of the STM image as a surface topography is generally sufficient on large distance scales. However, when interpreting an STM image with atomic scale resolution it can be enormously interesting due to the presence of localised surface electronic states associated with the surface atoms.

STM is a powerful tool for investigating atomically flat surfaces, such as a grid (see Appendix A) and graphite samples, with the atomic resolution able to look at the structural

configuration of the graphite atoms. Also the uniform atomic construction of graphite makes it a suitable sample to assess the quality of a freshly prepared STM tip.

The atomic surface of graphite was scanned using a STM, and the surface structure of graphite was observed as hexagonal layers, as consistent with the theory of the structure of graphite. Figure 3.5 shows hexagonal crystal structure of the graphite in the form of one layer.

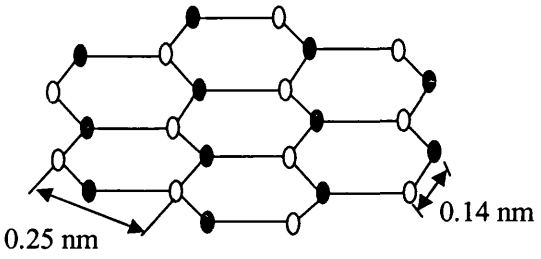

Figure 3.5: The hexagonal structure of a graphite layer[5].

The carbon atoms are organized in hexagonal layers which can be understood by observing the STM images of graphite. Therefore, mounting the graphite sample onto the STM head must be carried out precisely and the sample must not be touched by hand. Then, using the STM "Easy Scan" Software, the graphite surface is approached and imaged at scales, such as 50 nm^2. The image should show a clear atomic but if not then there may be a problem with the quality of the tip. Imaging is perfected by adjustment of the control parameters, i.e. moving to different locations, changing the scan size, z-ranging and zooming in on a flat area to try to achieve atomic resolution. Figure 3.6 shows an image of graphite that was obtained by the STM system.

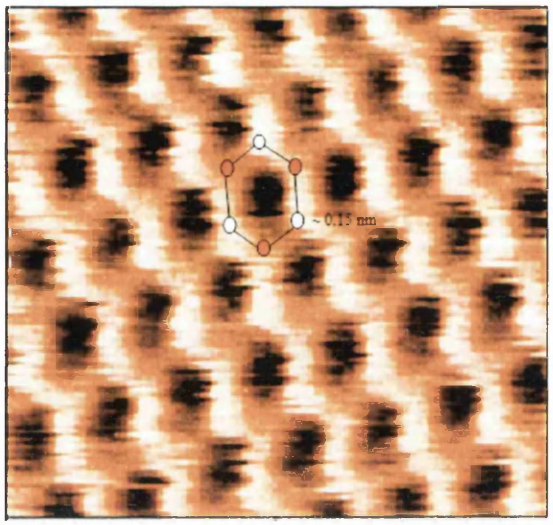

Figure 3.6: A ($1.26 \times 2.25\ nm^2$) image shows the regular arrangement of carbon atoms on the graphite surface recorded using constant current mode.

Interatomic spacing of carbon atoms in graphite[5] is known to be 0.14 nm and the measurements in figure 3.6 indicate spacing of 0.15 nm. In figure 3.6, the lattice appears hexagonal with a regular arrange. This indicates the STM system is precisely calibrated and can regularly used to test tip conditions.

3.5 Scanning tunnelling spectroscopy (STS)

3.5.1 Introduction

Scanning tunnelling spectroscopy (STS) studies the local electronic structure of a sample's surface. Of particular interest to our work is the use of STM as an instrument to perform spectroscopy on a variety of metal-semiconductor junctions. However, to do this, the relationship between the tunnelling current and bias voltage of the sample must be examined.

The sample bias voltage decides which electronic states can contribute to the tunnelling current[3]. It is this voltage dependence that forms the basis for the spectroscopic operation of the STM. Thus, a wealth of information on the electronic structure of the sample can be obtained in a spectroscopic mode of operation where the tip is held at particular position and the current against voltage measured (i.e. I-V curve). Hence, the I-V curves are characteristic of the electronic structure at a specific x,y location on the sample surface and can be set up to collect atomic information at every point in a data set thus providing a three-dimensional map of electronic structure.

3.5.2 Theory of STS

If the applied bias voltage is smaller than the work function of both tip and sample, the surface states around the Fermi level of the tip are expected to determine the tunnelling current and the tunnel current will take the form of equation 3.2.

$$I \sim \int_{E_F}^{E_F+V} \rho(r_t + E)dE \tag{3.2}$$

Equation 3.2 neglects the energy and potential dependence of the matrix elements, the tip density of states and the wave functions[3]. An additional barrier transmission coefficient *T(E,V)* is then included to take account of the voltage dependence on the surface wave functions. Hence, the tunnel current becomes;

$$I\alpha \int_{E_F}^{E_F+V} \rho(E)T(E,V)dE \tag{3.3}$$

In order to achieve a relationship with the density of states, Feenstra *et al*[6]demonstrated that by normalising the differential conductivity (*dI/dV*) by the total

conductivity *I/V,* provides a quantity corresponding to the normalised density of states. The derivative is calculated as

$$dI/dV \alpha e\rho(eV)T(eV,eV)+e\int_0^{eV}\rho(E)\frac{d}{d(eV)}[T(E,eV)]dE \tag{3.4}$$

The normalised conductivity is given to be equation 3.5

$$\frac{dI/dV}{I/V}=\frac{\rho(eV)+\int_0^{eV}\frac{\rho(E)}{T(eV,eV)}\frac{d}{d(eV)}[T(E,eV)]dE}{\frac{1}{eV}\int_0^{eV}\rho(E)\frac{T(E,eV)}{T(eV,eV)}dE} \tag{3.5}$$

Feenstra[6] argued that since transmission probability terms *T(eV,eV)* and *T(E,eV)* appears as ratios in the second term of the numerator and denominator of equation 3.5, that their dependence on separation and applied bias tend to cancel. Therefore, the normalisation reduces to equation 3.6, which is equivalent to the normalised surface density of states.

$$\frac{dI/dV}{I/V}\equiv\frac{d\ln I}{d\ln V}\approx\frac{\rho(E)}{\frac{1}{eV}\int_0^{eV}\rho(E)dE} \tag{3.6}$$

Where the $\rho(E)$ is the surface density of states and the denominator of the equation 3.6 is the normalisation factor.

3.6 Summary

This chapter has outlined the basic principles of the STM operation along with its spectroscopic counterport STS. This understanding is necessary to develop the STM into a BEEM instrument and the principles of BEEM are discussed in such a context in the next chapter.

3.7 References

[1] G.Binning, H.Rohrer, Ch.Gerber, and E.Weibel, Phys. Rev. Lett, **49, 57**(1982).

[2] A.P. French and E.F. Tayler ,"An Introduction to Quantum Physics", Chapman and Hall(1994).

[3] J.Tersoff ,N.D. Lang ,"Methods od Experimental Physics : Scanning Tunnelling Microscopy"Chapter1,**1-3**,Edit.J.A. Stroscio and W.J. Kaiser , Academic Press (1993).

[4] A. Bryant, D.P.E. Smith, C.F. Quate, Appl. Phys. Lett. **48**, 832 (1986).

[5] Easy Scan STM system hand book.

[6] R.M Feenstra, J.A. Stroscio, and A.P. Fein, Surf. Sci, **181**, 295 (1987).

Chapter 4

Ballistic Electron Emission Microscopy (BEEM)

4.1 Introduction

As discussed in previous chapter, scanning tunnelling microscopy (STM) is a quantum mechanical tunnelling process between two electrodes, usually a sharp metal tip and a sample. It has proved extremely valuable for use in both spectroscopy and imaging, and has the capability to characterise the surface topography and the electronic structure at atomic-scale resolution. Along with the many exciting applications of STM, ballistic electron emission microscopy (BEEM) has recently become well-known as a technique in its own right. This technique was invented in 1988 by W. Kaiser and D. Bell[1,2] and is currently in use in many laboratories. BEEM is a technique based on STM, but is three terminal measurements instead of the normal two. This chapter details how BEEM can be used to investigate buried interfaces between, for example, a metal layer and semiconductor substrate, with nanometre resolution and enables energy spectroscopy of electron transport.

BEEM uses the STM tip as an injector of 'hot' electrons into a metal-semiconductor sample. The tip-metal-semiconductor arrangement consists of three electrodes separated by various interfaces. The multi-electrode system is achieved with sample via an electrical contact to the top metal and also on the back contact (an Ohmic contact is required on the semiconductor back surface). Figure 4.1 displays the corresponding energy diagram of emitter, base, and collector. For the case of a Schottky barrier formed by a metal-semiconductor contact, the metal layer acts as a biasing electrode and the semiconductor as a collector of hot or ballistic electrons.

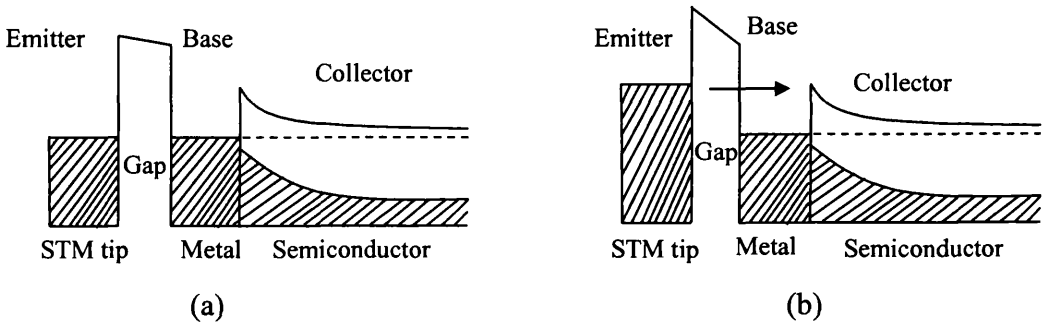

Figure 4.1: An energy band diagram for BEEM on a metal semiconductor Schottky interface (a) Applied tunnel voltage of zero, and (b) Applied tunnel voltage greater than the Schottky barrier.

When the STM tip is negatively biased, electrons tunnel across the vacuum air barrier from the tip into the metal contact. If the metal contact is earthed then many of electrons will conduct to earth, undergoing energy relaxation and scattering in the process. However, some electrons will reach the interface and their energy will dictate if they are able to overcome the Schottky barrier. If they do then they are referred to as 'hot' electrons. As the voltage between the tip and sample is varied, the hot electron's energy distribution is controlled and ballistic electron emission spectroscopy (BEES) of the interface can be performed. Figure 4.2

shows the BEEM spectra which can be obtained by using the BEES technique. Moreover, when the tunnel voltage is less than the Schottky barrier height, no electrons will have enough energy to conduct over the barrier and the collector current will measure zero amps. As the voltage is increased to a level higher than the barrier, some of the electrons will have the energy to cross the interface into the semiconductor and a collector current will be established.

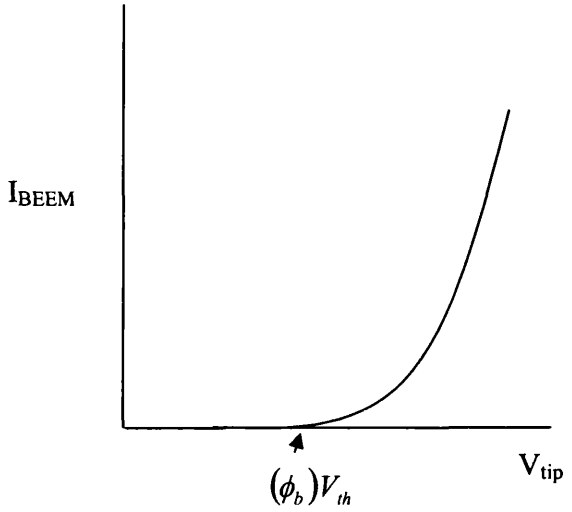

Figure 4.2: Example of a theoretical (I-V) characteristic for BEEM, displaying a threshold voltage, V_{th}, equal to the interfacial Schottky barrier, ϕ_b.

4.2 Three contact measurements of BEEM

Conventional STM is performed using two contact terminals, i.e. the tip and sample. BEEM however is a three terminal modification of STM. It is a powerful low-energy tool for nanometre scale local characterisation of buried metal-semiconductor interfaces. The STM metal tip injects, via tunnelling, electrons across the vacuum barrier into the metal contact layer deposited on a semiconductor. The STM tip plays the role of a local electron gun that takes advantage of tunnelling to achieve two important conditions, electrons tunnel through a

very small area in the metal and electrons can be positioned in energy between the semiconductor Fermi level and the Schottky barrier, ϕ_b. The second terminal connection in the BEEM system is the sample's metal top contact, which is connected to earth. A third terminal on the samples back (Ohmic) contact is used to collect the hot electrons which pass across the metal semiconductor interface, this focuses the BEEM (or collector) current. In this study, the metal back contact is an ohmic nickel contact, prepared as discussed in chapter 2 and chapter 5.

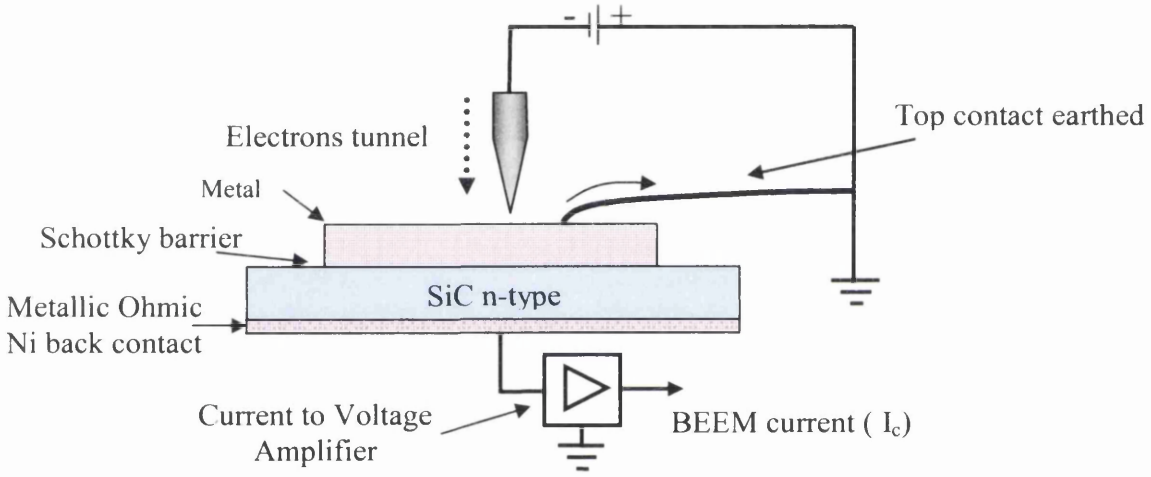

Figure 4.3: A schematic of the BEEM experimental set-up with three contacts.

A schematic of the BEEM experimental set-up with three contacts is illustrated in figure 4.3, where BEEM is used to study a metal-semiconductor Schottky contact. Furthermore, the BEEM technique can be regarded in some ways as a filter for the tunnel electrons at the semiconductor interface, since only hot electrons can pass over the Schottky barrier to be collected from the back contact as a BEEM current. Clearly the metal layer thickness is important and should be approximately equal to, or less, than the mean free path of the probing electrons, so that they can reach the interface with minimal scattering. Note

that, the majority of tunnel electrons will see the base terminal (i.e. the top contact) as the easiest way to the earth.

When the tip bias voltage is greater than the Schottky barrier at the metal-semiconductor junction a small fraction of electrons will have enough energy to pass through the barrier. They then move ballistically through the semiconductor until they thermalise and are then collected in the collector (or BEEM) current.

In order to perform BEEM experiments with an STM, generally three further requirements should be fulfilled. Firstly, the semiconductor and the metal have to be contacted separately. Then, the BEEM current must be measured as the back contact connected to a current amplifier. Finally, the metal top contact has to be grounded. The BEEM set-up requires good electrical performance to measure the current with a noise level less than 1 pA. These wire electrical contacts need to be shielded and the amplifier circuit also has to be located close to the Schottky sample's connection to reduce and eliminate pickup of electrical noise. A schematic band diagram for BEEM is shown in figure 4.4. The energy and the hot electron distribution can be controlled in the semiconductor structure by changing the tip voltage, V_T.

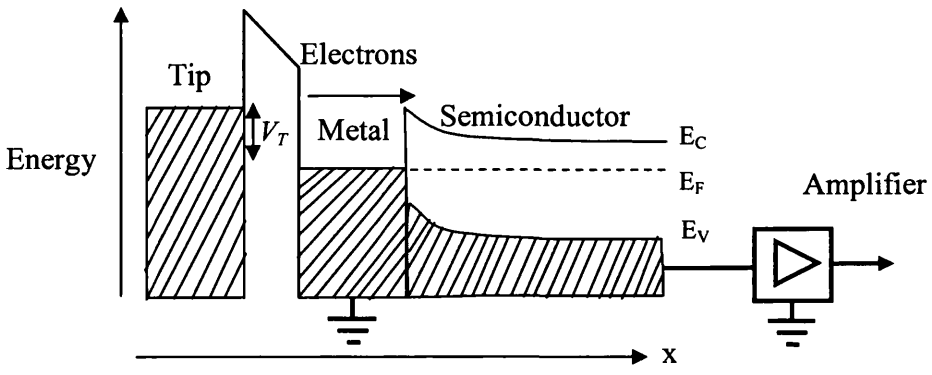

Figure 4.4: A schematic band diagram for BEEM.

4.3 Ballistic electron emission spectroscopy (BEES)

4.3.1 Introduction

Ballistic electron emission spectroscopy can be used to obtain local information of the interface in different positions by taking a normal localised I-V spectrum with the STM, but monitoring the result at BEEM current as a function of voltage rather than the tunnel current. Hence, the BEES technique records the BEEM current as the function of the applied tip bias voltage, as illustrated in figure 4.2, which gives a threshold voltage.

In addition by taking a number of readings for the same point in order to acquire an average of the data helps to smooth out the variations due to noise.

4.3.2 Theory of BEES

In order to record a BEEM spectra, the STM tip is maintained at a fixed x-y position while the tunnel voltage (V_T) is swept within a chosen voltage range. The ballistic current, which depends on tip voltage, V_T, and tunnel current, I_T, is measured at this position in constant current mode. In addition, to quantify the threshold voltages and to investigate the detail of BEEM spectra (I-V curves), the experimental data can be fitted using a theoretical model proposed by Bell and Kaiser[2] for the collector current, I_c. This model assumes a constant tunnel current, I_T, and is known as the BK model. The expression for I_c is giving by;

$$I_C(V_T) = R \frac{\int_{E_{min}}^{\infty} D(E_z)dE_z \int_0^{E_{max}} f(E_z + E_t)dE_t}{\int_0^{\infty} D(E_z)dE_z \int_0^{\infty} [f(E_z + E_t) - f(E_z + E_t + V_T)]dE_t} \qquad (4.1)$$

Where E_z and E_t are the energies associated with the component of the electron momentum normal and transverse to the metal-semiconductor interface, respectively, $D(E)$ is the tip-metal tunnelling probability, $f(E)$ is the Fermi-Dirac distribution, E_F is the Fermi energy in the tip, m_e is the free electron mass, m_e transverse effective electron mass, and R is a scaling factor. The integration limits, E_{min} and E_{max} are $E_{min}= E_F - q(V_T-V_{th})$ and $E_{max}= [E_z-E_F+ q(V_T-V_{th})]\, m_e /(m_e -m_t)$.

The BK model theory was used for fitting of single threshold ballistic electron spectra in this work, discussed later on in chapter 6.

4.4 BEEM survey of literature

Since the work of Kaiser and Bell[1], the application of BEEM to various semiconductor surfaces and interfaces has already produced many interesting results. BEEM has been used to observe and investigate the local interface band structure and the important features of the conduction band of Au-Si and Au-GaAs[1]. The first typical $I_c - V$ BEEM spectrum was obtained for the Au-Si junction at a tunnelling current of 0.87 nA, as shown in figure 4.5.

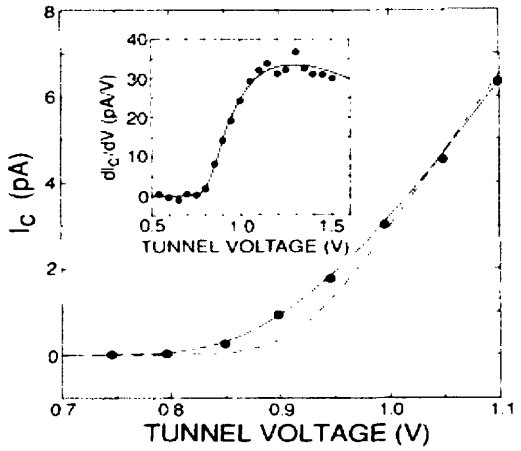

Figure 4.6: BK model was applied to experimental data from Au-Si[1].

The agreement of the theory with the experiment when the derivative dI_c/dV vs V is plotted, can be seen as shown in the in-set on figure 4.5. BEEM has been developed to study the magnitude of the transmitted current into the substrate which depends strongly on the local properties of the interface[3,4]. The capability of BEEM to probe the electronic properties of semiconductors on the local scale has also been demonstrated on systems including InAs/GaAs[5] and SiGe strained layers[6]. In these cases, the BEEM technique, which was first used to probe the Schottky barrier on a local scale, has been successfully used to study the electronic properties of buried heterojunctions[2]. BEEM was also successfully applied to metal –insulator –semiconductor structure to study the transport related to oxide properties on a microscopic scale in buried CaF_2/Si[7]and SiO_2/Si[8].

Metal contacts to semiconductor materials have been investigated using BEEM to study the local Schottky barrier of interface, for example contacts to GaP[9], GaInP[10,11], GaAsN[12] and SiC[13,14]. Of obvious interest with regard to this current study were previous BEEM investigations[13] on 4H-SiC and 6H-SiC. Kacze, Pelz, Chen, and Choyke[13,14] studied Pd and Pt Schottky contacts on 6H- and 4H-SiC and also Pd Schottky contacts on 15R-SiC. It was shown that in the contacts to 4H-SiC, there is additional information related to the conduction band structure. In their work, I-V characteristics are similar to the Bell-Kaiser (BK) model, but can be fitted with multi-thresholds due to the electronic nature of 4H-SiC. In order to determine the Schottky barrier height precisely for Pd, BEEM spectra are averaged together to reduce the noise interference, as seen figure 4.6.

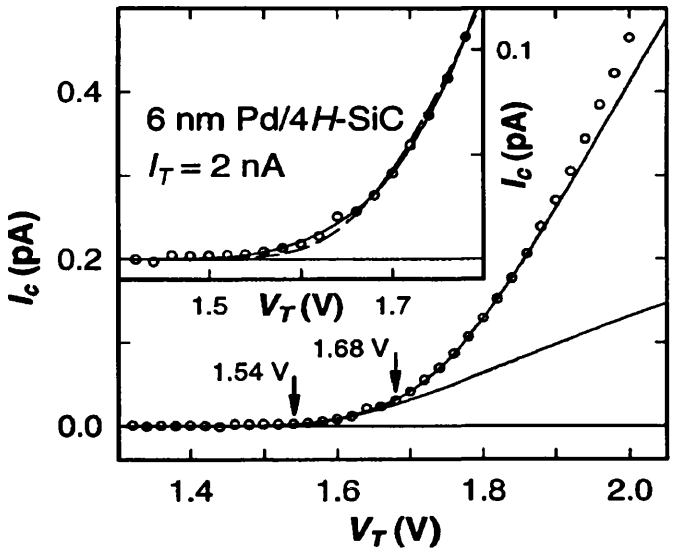

Figure 4.6: I_c-V_T curves for Pd Schottky contacts on 4H-SiC [14].

As it has been mentioned in previous section, BEEM is used to investigate the local Schottky barrier heights by directly determining the threshold voltage V_{th}, above switching BEEM current is observed.

In our work, BEEM has been developed to investigate the electronic properties and localised Schottky barrier heights of the interface between Ni and (4H)SiC, and results are presented in chapter 6, sections 6.6 to 6.9. Details of the experimental set-up can be found in the following chapter.

4.5 References

[1] W.J. Kaiser and L.D. Bell, Phys. Rev. Lett. **60**, 1406 (1988).

[2] L.D. Bell and W.J. Kaiser, Phys. Rev. Lett. **61**, 2368 (1988).

[3] L.D. Bell, W.J. Kaiser, Annu. Rev. Mater. Sci. **26**, 189 (1996).

[4] Fernandez, H.D. Hallen, T. Huang, R.A. Buhrman, J. Silcox, Appl. Phys. Lett. **57**, 2826 (1990).

[5] R.H. Williams, Appl. Surf. Sci. **70-71**, 386 (1993).

[6] L.D. Bell, A.M. Milliken, S.J. Manion, W.J. Kaiser, R.W. Fathauer, W.T. Pike, Phys. Rev. B **50**,8021 (1994).

[7] M.T. Cuberes, A. Bauer, H.J. Wen, M. Prietsch, G. Kaindl, J. Vac. Sci. Technol. B **12**,2646 (1994).

[8] R. Ludeke, A. Bauer, E. Cartier, Appl. Phys. Lett. **66**,730 (1995).

[9] Bauer, M.T. Cuberes, M. Prietsch, G. Kaindl, Phys. Rev. Lett. **71**, 149 (1993).

[10] J.J. O'Shea, C.M. Reaves, S.P. DenBaars, M.A. Chin, V. Narayanamurti, Appl. Phys. Lett. **69**,3022 (1996).

[11]M. Kozhevnikov, V. Narayanamurti, A. Mascarenhas, Y. Zhang, J.M. Olson, D.L. Smith, Appl. Phys. Lett. **75** ,1128(1999).

[12] M. Kozhevnikov, V. Narayanamurti, C.V. Reddy, H.P. Xin, C.W. Tu, A. Mascarenhas, Y. Zhang, Phys. Rev. B **61**, R7861(2000).

[13] H.-J. Im, B. Kaczer, J.P. Pelz, W.J. Choyke, Appl. Phys. Lett. **72**,839 (1998).

[14] B. Kaczer, H.-J. Im, J.P. Pelz, J. Chen, W.J. Choyke, Phys. Rev. B **57** , 4027 (1998).

Chapter 5

Instrumentation and Development

5.1 Introduction

In this chapter an outline of the key instrumentation and experimental developments are discussed. The chapter starts with a description of the system's design, which has been modified precisely for suitable BEEM measurements. In fact, the modification of the sample holder was based on the initial work done by an MPhys student (Mark Holton) of the Physics Department, and basic amplifier circuits built in a final year project by an undergraduate student in the Department of Electrical Engineering. Furthermore, the modifications development and testing of revised amplifier circuits are discussed within this chapter, focussing on the amplification of pA currents and considering the elimination of the electrical noise. Note that the primary amplifier is based on the successful work of PhD student (Mathew Ackland[1]), who used a similar set-up for measuring near-field generated photo-currents. The preparation of Ni-SiC Schottky samples is addressed within this chapter

including macroscopic I-V measurements. The final experimental set-up is discussed with modifications and three terminal connections explained.

5.2 The design of the system

5.2.1 The sample holder

In order to study Schottky samples the BEEM experiment requires a small sample holder to fit into a desktop STM system. The Schottky diode sample ($5\ mm \times 5\ mm$) is located under the clamp and is held in that position by bringing the clamp down to make an electrical contact with the back contact. The sample holder was made from different types of materials, including Tufnell (insulating), gold and brass as shown in figure 5.1. In order to detect a BEEM current three electrical connections are necessary, the top contact, Ohmic back contact and STM tip. The top electrical contact made from gold wire, was bent over at the end to act as a probe and the apex end was etched to be as thin as possible.

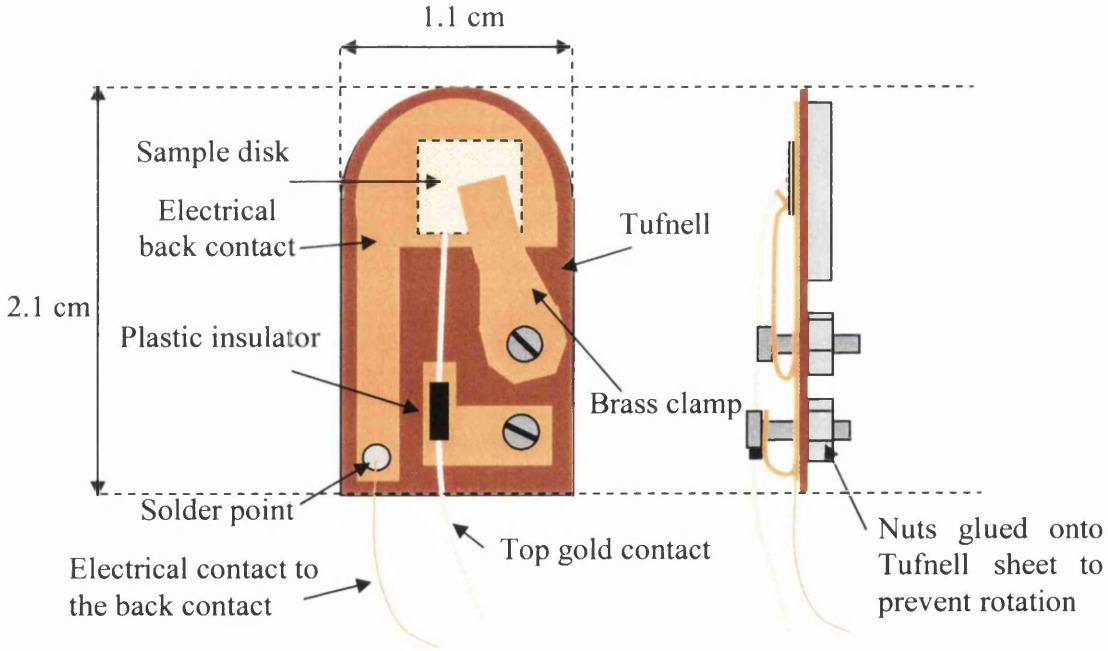

Figure 5.1: A three contact sample holder.

The top contact which has an insulating plastic cover is also placed into another brass device that allows it to act as a clamp. The top contact's clamp allows the top contact to be gently lowered to make electrical contact with a nickel dot, without penetrating directly through the Ni layer to the SiC substrate beneath. Therefore, the sample holder consists of two sensitive terminal connections, gold wire as a top contact and copper wire as a back contact. The two contacts have to be as short as possible and in order to reduce the level of noise interference. Due to the difficulty of using an unshielded wire with the STM drum.

5.2.2 The sample holder with a STM unit

The sample holder, which was especially designed to fit vertically, is attached to the STM magnetic drum head as shown in figure 5.2. The drum is then automatically approached towards the tip by the Z-stepper motor until the tunnelling current is achieved, during the STM's automatic approach procedure.

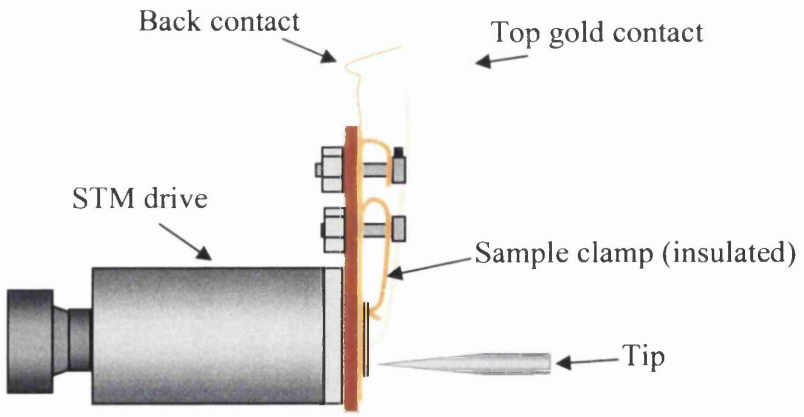

Figure 5.2: The sample holder attached to STM drum.

The ends of the top and back contacts were connected to the Keithley 2400 Source –ammeter and 6485 Pico-ammeter via a screwable connection block to check the I-V measurements of the Schottky contact and also to ensure a good contact on the thin nickel Schottky layer prior to commencing the BEEM imaging procedure. Note, it is imperative to check the quality of the delicate electrical contacts with the sample after installation with the STM system as degradation of a single contact would compromise the entire BEEM imaging technique. Particular attention must be paid to the delicate connection with the thin Ni top contact layer, as this is susceptible to pierce directly through the Ni layer to the SiC substrate.

In order to protect the whole system from electrical interference, magnetic interference and air movement, the sample holder and STM head unit should be kept in an earthed faraday cage. In this study, a sealed metal computer desktop case was used as a faraday cage. The Pico-ammeter was used to monitor the BEEM current before connecting the Schottky sample to the amplifier circuit, described in detail in the following sections. In addition, figure 5.3 illustrates the connection of the BEEM to the Pico-ammeter in order to observe low currents (pA) and to check the capability of generating a low current from the Schottky contact system.

It is important to note that average BEEM currents were displayed on the Pico-ammeter's screen, ranging from approximately 0.5 pA to 30 pA. The maximum current was detected in the active regions of BEEM and this method was used to find a BEEM area and to check the connections.

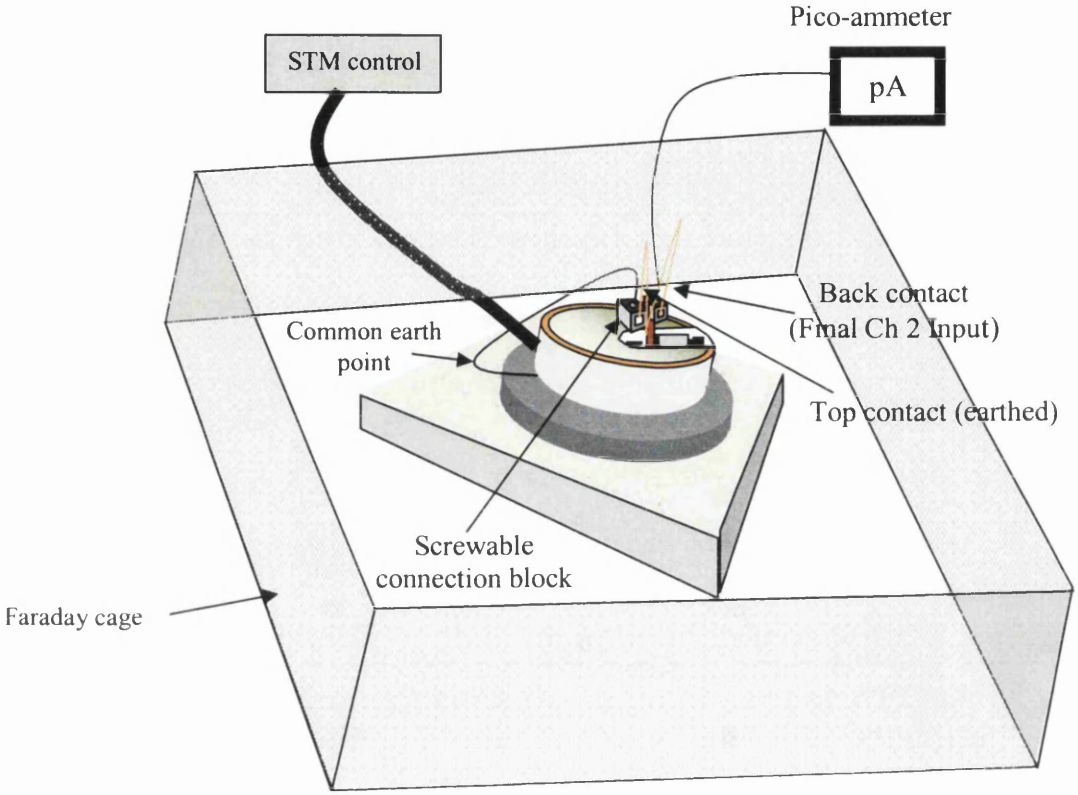

Figure 5.3: The STM and sample holder inside a faraday cage.

5.3 Electronics

5.3.1Three stages amplifier circuits

The BEEM currents are usually low, typically in the order of ~ pA, in fact it is virtually impossible to measure BEEM signals and create an image without amplifying the signals. The current which is generated in BEEM process needs to also be converted to voltage (for input into the auxiliary input on the STM controller) and thus amplification and I-V conversion is necessary. This could be achieved by using an I-to-V amplifier circuit, however, the amplifier would need to have a gain of the order of 10^{12} in order to turn 1 pA to

1 *V*. Figure 5.4 displays the first stage amplifier with 10^7 gain, and is based on the Analogue Devices AD549 ultra-low input bias current operation amplifier[2]. The amplifier circuit was designed with sensitivity of the order of femto-amps.

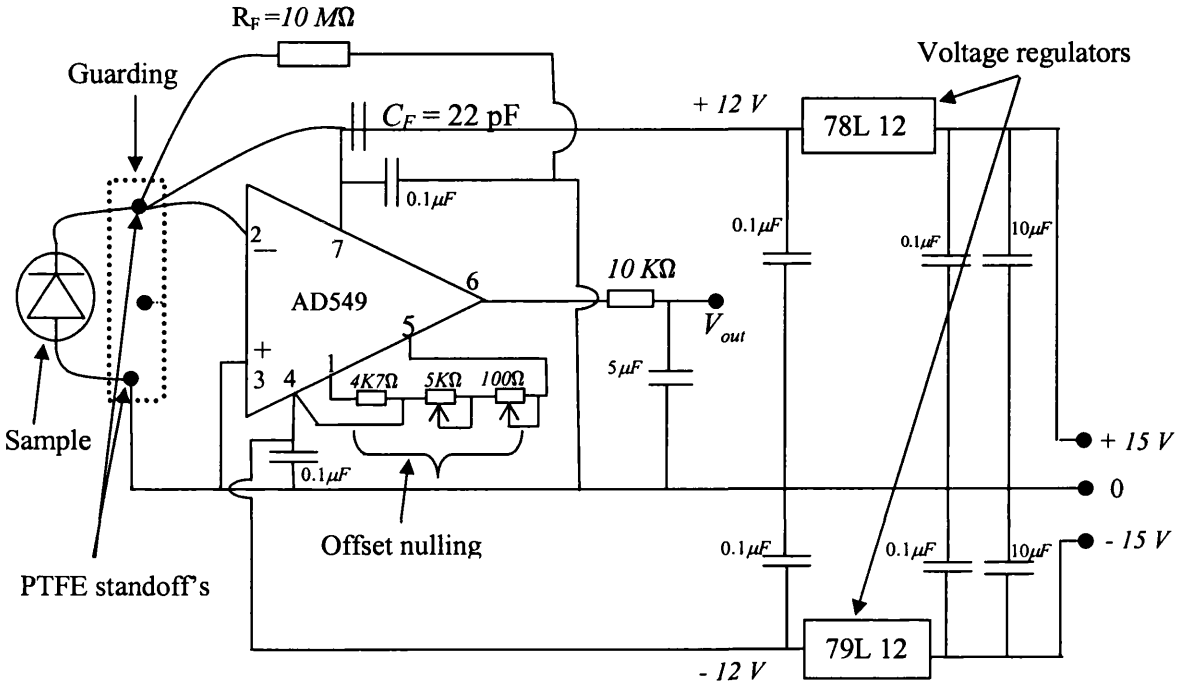

Figure 5.4: 1st stage I/V converter amplifier circuit, with 10^7 gain.

When the connections to the sample were checked, the back and the top contact leads were connected to an earth and an amplifier circuit, respectively. The preamplifier was connected to the sample by a very short shielded cable via PTFE standoff's to prevent parasitic leakage currents from the printed circuit board.

The AD549 amplifier is a very sensitive device and needs a stable power source, it is therefore operated by two banks of rechargeable batteries providing a stable $\pm 15\,V$. The batteries are connected to the AD549 amplifier by positive (78L12) and negative (79L12)

voltage regulators with additional smoothing capacitors ($0.1\mu F$). They work to stabilise the input voltages to $\pm 12\,V$ prior to the amplifier. The resistor R_F (10 MΩ) is used to determine the feedback of the circuit and the capacitance C_F (22 pF) is used as a low pass filter to determine the cut off frequency which is greater than the scan frequencies.

For further amplification to bring a pico-ampere current up to the level of around 1 V, a further two stages are required. This increases the gain of the circuit to 10^{12}. Figure 5.5 and figure 5.6 illustrate the second and the third stages of amplification with changeable gains 10^3 and 10^2, respectively.

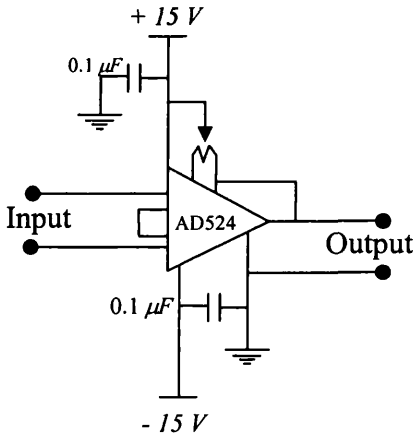

Figure 5.5: 2nd stage amplifier circuit, with 10^3 gain.

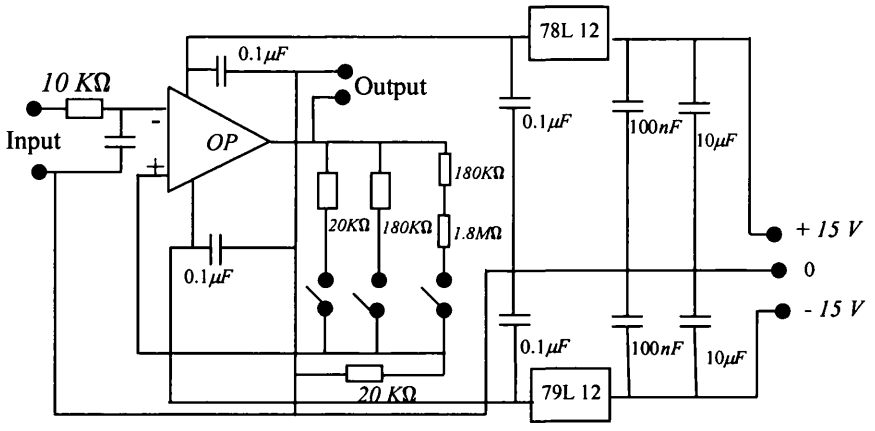

Figure 5.6: 3rd stage amplifier circuit, with 10^2 gain.

5.3.2 Testing the circuit and the channel 2 input on the STM

The amplifier circuits can be tested in different ways. In this study, two methods have been used. For the first method, the three circuits were connected together and configured to a gain of 10^9 .They were then connected to the small test circuit which can generate 1 nA, as shown in figure 5.7.

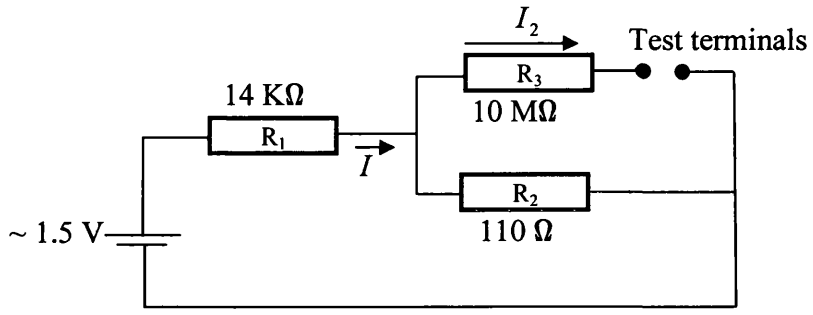

Figure 5.7: Amplifier test circuit.

$$I = \frac{V}{R_{total}} \tag{5.1}$$

$$R_{total} = R_1 + \frac{1}{R_2 + R_3} \tag{5.2}$$

According to eq. (5.1) and (5.2) and the voltage shown in figure 5.7

$I = 1.07 \times 10^{-4} A$

and thus $I_2 = I\frac{R_2}{R_2 + R_3} = 1.17 \times 10^{-9} A \approx 1nA$

Experimentally, when the test circuit was then connected to the amplifier circuits, the amplifiers produced an output of 1.01 V, so at this current (nA) the amplifiers were working.

The second method which was used to test the sample connection and amplifier circuits used the Schottky diode sample, a torch and oscilloscope, as presented in figure 5.8. This method allows the current behaviour as function of illumination to be detected and also allows the offset voltage to be modified in dark conditions to prevent saturation. The Schottky diode sample is sensitive to light and this can be used in testing the amplifier to prove the quality of both the sample and the circuit. In BEEM, the diode and the amplifier circuit work in reverse bias.

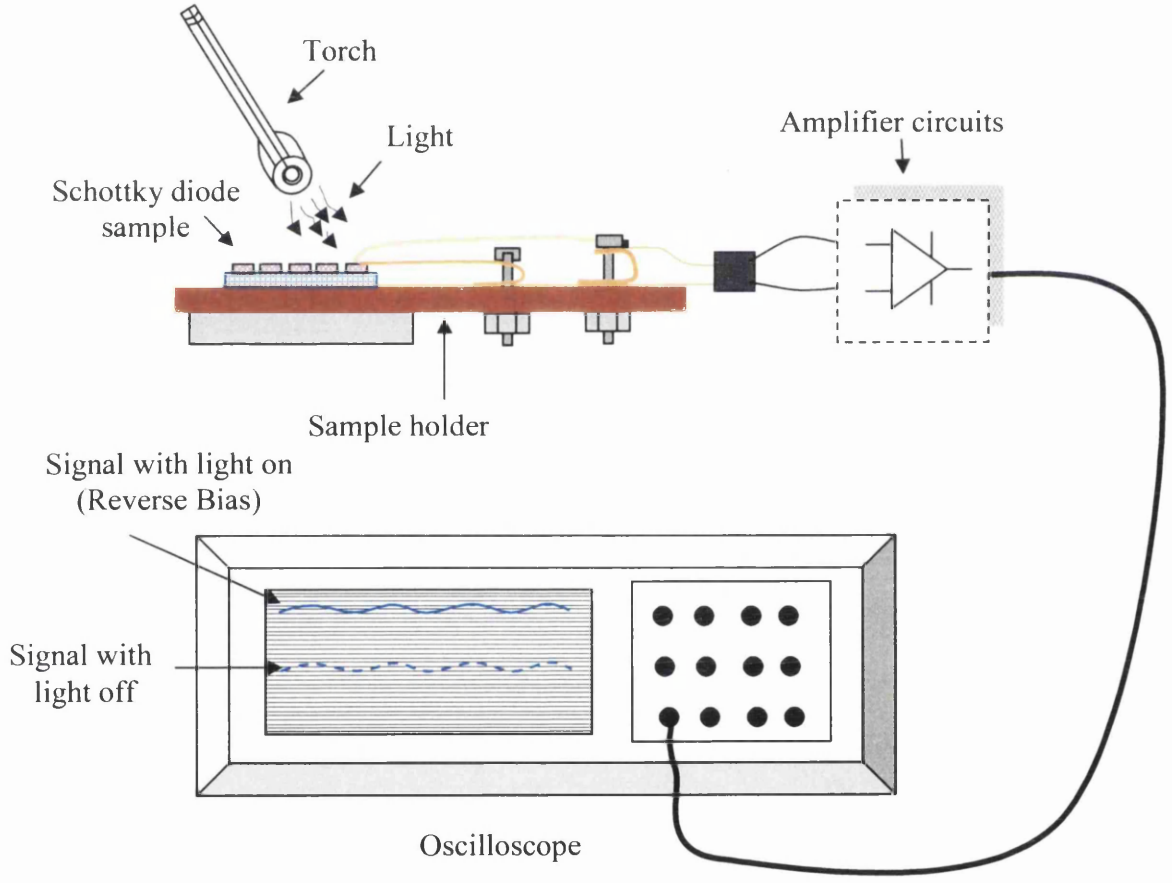

Figure 5.8: Schottky diode sample connected to an amplifier and an oscilloscope.

The three stages amplify with a gain of the order of 10^{12} and can maximize the pico-ampere current to $1V$. This voltage then enters into a channel 2 input ($0 - 10V$) of the STM and can be imaged as BEEM current with a Z-output image simultaneously. It is important to note that the voltage offset of the amplifier is necessary when dealing with different samples which have different I-V characteristics.

In order to measure the low current, a very small offset voltage is needed in a dark area where the experiment is placed. Therefore, the first stage amplifier consists of offset variable resistances, 4.7 KΩ, 5 KΩ and 100Ω and they are connected in series. The 5 KΩ is used for crude offset balancing and the 100Ω potentiometer is used for fine-trimming.

5.4 Sample preparation

5.4.1 Ni-SiC Schottky diodes

In this study, the BEEM investigation of Schottky barriers was focused on nickel contacts with silicon carbide. Schottky diodes were fabricated specifically for BEEM imaging, with particular focus on the accurate deposition of uniform thin Ni top contacts.

The basic sample structure consisted of a silicon carbide substrate with a 10μm thick n-type epilayer doped with nitrogen at a concentration of 10^{16} cm^{-3}. The Ni back contact was deposited using an Edwards evaporator, and the back Ni-SiC interface was annealed at a temperature of 900 to1000°C for 10 minutes to make it Ohmic in nature[3,4]. The Schottky Ni top contacts were deposited through a razor foil which acted as a mask, with a nickel flux of 60 Å /s to produce circular contacts of about 600 μm in diameter. The SiC surface contains a certain density of surface defects that, when incorporated in Ni-SiC interfaces provide a current leakage path dominating the device characteristics, and can result in Ohmic behaviour

of the junction. Figure 5.9 shows the basic structure and the top view of a Ni-SiC Schottky contact.

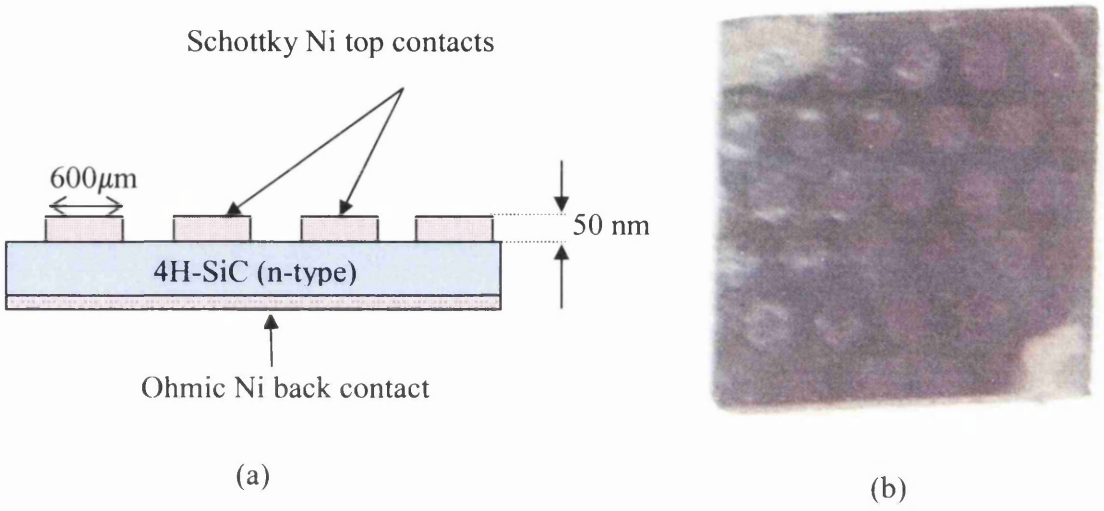

Figure 5.9: (a) The basic structure of a Ni-SiC Schottky diode contact, and (b) the top view of a real Schottky sample.

The SiC wafer surface was processed by a progression of ex-situ cleaning and etching steps to produce an atomically clean surface appropriate for the growth of good electrical contacts. The cleaning methods comprised of a solvent clean, a piranha clean, and an RCA clean. The solvent clean uses trichloroethylene, acetone, iso- propanal and methanol to gently remove oil based contaminants and dust from the wafer surface. The piranha clean uses sulphuric acid and hydrogen peroxide to further remove organic substances. The RCA cleaning method is harsher and chemically removes ionic contaminants, organic substances and strips surface oxides by etching the SiO_2, leaving the SiC surface untouched and atomically clean and flat . The cleaning method is listed in Appendix B.

5.4.2 Contact deposition: Edwards evaporation chamber

The thick Ni back contact was applied using an Edwards E306A thermal evaporator which operated at a pressure in the 10^{-7} millibar range, which was achieved using rotary and diffusion pumps. The Edwards system achieves metal evaporation by E-beam bombardment using a tungsten coil filament to irradicate small pieces of pure nickel within a graphite crucible. Typically the filament current is 80 mA and the crucible is at a potential of 2.5KV. The sample is located approximately 30 cm directly above the Ni source oriented with the side to accept Ni deposition facing downwards, as seen in figure 5.10. For back contact deposition the sample is fixed by two small clips at opposite corners leaving the SiC face open to Ni deposition. A moveable shield is inserted between the crucible and sample which, when in position, shadows the sample from the evaporating Ni flux, and is translated out of the flux path to control the Ni deposition time. The metal evaporation rate, or Ni flux, is measured by an in-situ crystal monitor, and once the desired constant flux is attained the shield is translated away to start deposition. The deposition rate is controlled by the filament current and crucible potential, and measured using a calibrated crystal monitor, thus the deposited layer thickness is subsequently controlled by the deposition time.

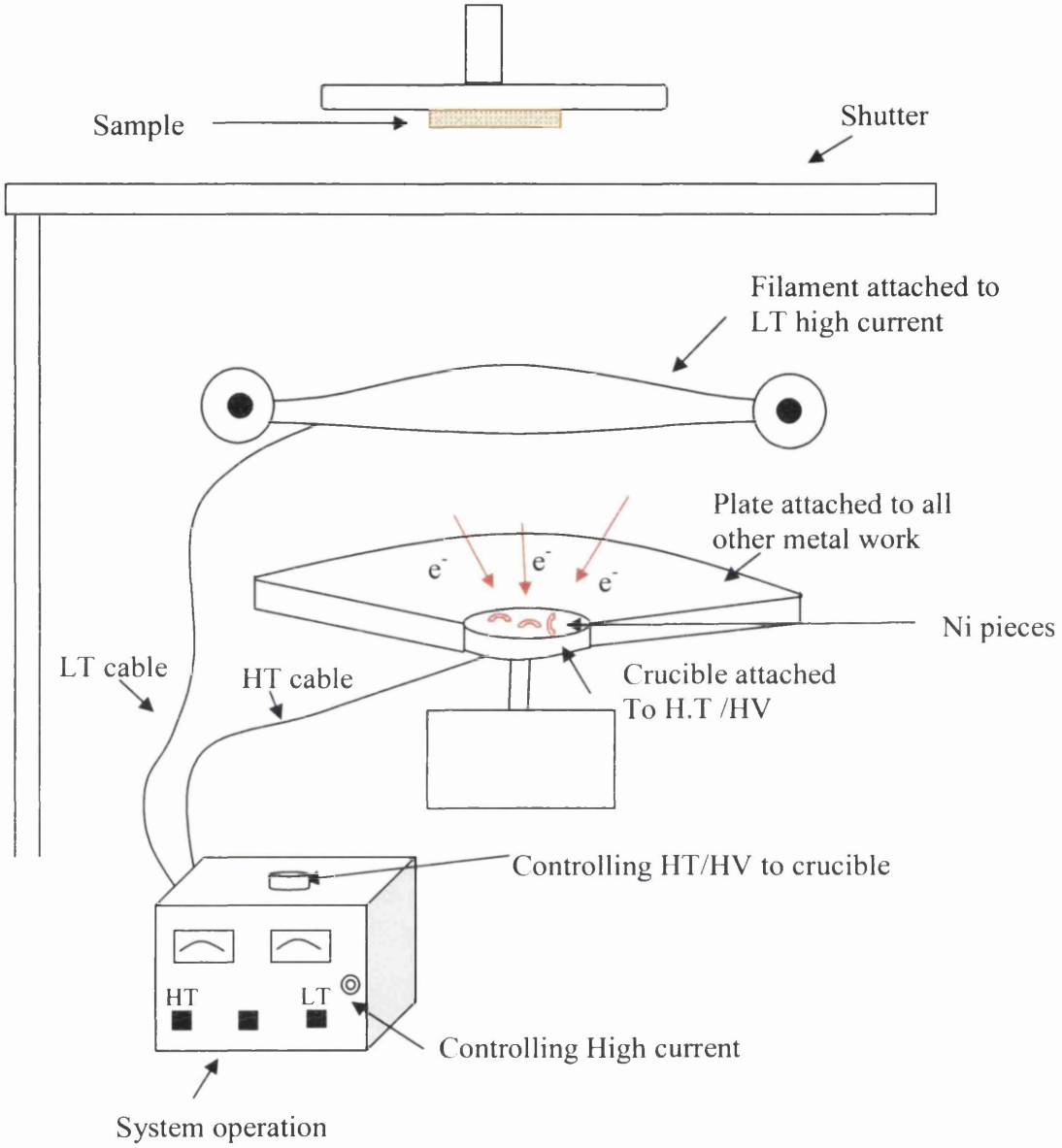

Figure 5.10: The HV on the crucible combined with the LT/high current on the filament bombards the sample with electrons melting the metal in the crucible.

Thin layer deposition was achieved by establishing a very low steady flux rate, only possible after the initial melting of the small Ni pieces within the crucible. Once a stable flux was achieved the sample shield was removed for very short deposition times, typically 20sec to 1min. However this process was dependant on the accuracy of the crystal monitor in

measuring the Ni flux, which proved to be a very unreliable technique, resulting in a hit or miss nature. Lastly, the sample was annealed at 1000^0C for 10 minutes to make the back contact ohmic in nature.

5.4.3 Contact deposition: UHV evaporation system

The top contacts (nickel dots) were applied using the UHV evaporation system, without subsequent annealing. In the UHV system, as in the Edwards evaporator, the top contact was deposited through a tightly fitted mask which mounted the sample onto a sample holder stub top-plate. When working under UHV conditions cleanliness is imperative, hence the stub top-plate and mask were cleaned via an Aqua Regea etch consisting of a 3:1 mixture of nitric acid to sulphuric acid for a duration of 2mins. Following that the mask and top plate were admitted to UHV (without sample) and degassed by e-beam bombardment using a previously degassed filament at 2.7A and an accelerating potential of 2kV. The sample mounting stub was then removed from vacuum and the freshly cleaned sample (solvent clean and HF dip) was clamped beneath the mask, and subsequently installed into vacuum. Prior to UHV deposition the sample was heat treated in vacuum by e-beam bombardment to a temperature of 900°C. This removed oxygen from the sample surface and simultaneously annealed the earlier deposited back contact to an ohmic nature. Ni contact deposition was performed with the sample oriented as in the Edwards system and in the same way using a shield system to control the deposition time. Metal was evaporated using an Oxford Research EGN4 mini e-beam UHV evaporator. Nickel of 99.99% purity was deposited at a rate of 1Å in 7sec, and consequently a 50 nm thick top contact was deposited in one hour. The benefit of depositing metal contacts in such a system, apart from the high level of cleanliness, is the

fine control of the evaporation procedure and the accuracy in depositing specifically thin layers, which is a result of accurate source calibration.

5.5 I-V Measurements

Current-voltage (I-V) relationships investigate the electrical characteristics of 4H-SiC Schottky rectifiers with nickel contacts[5]. The measurement of current –versus- voltage curves (I-V) is one of the most important and widely applied techniques for characterising contacts to semiconductors. The current is measured as a function of voltage and then the I-V measurement data can be fitted according to equation 2.6 (see chapter 2) in the form of a ln(I) versus V plot as written by,

$$\ln(I) = \frac{e}{nk_BT}V + \ln(I_0) \tag{5.3}$$

and the ideality factor (n) can be calculated from the gradient of the graph. Moreover, using equation 5.4, the Schottky barrier can be calculated.

$$I_0 = A^*T^2 \exp\left(\frac{-e\phi_b}{k_BT}\right) \tag{5.4}$$

During this work, several samples were used which all consisted of a silicon carbide substrate, with annealed nickel back contact and with dots evaporated onto the silicon carbide surface. I-V measurements were carried out to determine the Schottky barrier height values experimentally using Pico-ammeter and Source-ammeter, as illustrated in figure 5.11.

Diagram 5.11(a) shows the experimental configuration used in measuring the I-V characteristics. A contact probe is brought down onto the thin nickel top contact layer, then,

the top contact is connected to a voltage Source-ammeter and the back contact is connected to a Pico-ammeter in series. As a result of this connection, a voltage and current response is recorded and then plotted, as indicated in figure 5.12.

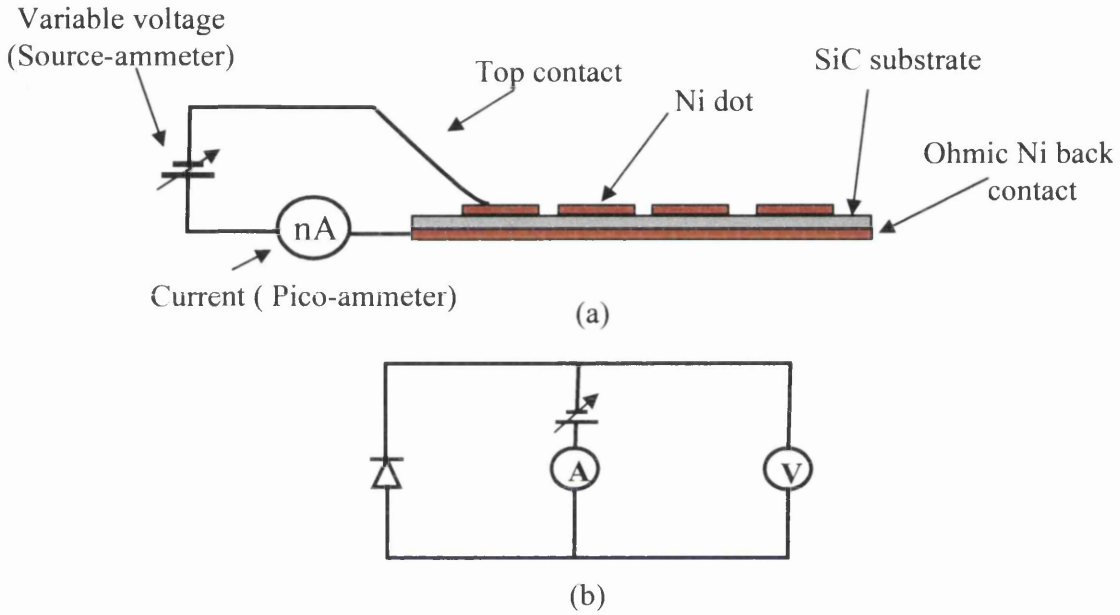

Figure 5.11: (a) I-V technique diagram, and (b) Its equivalent circuit.

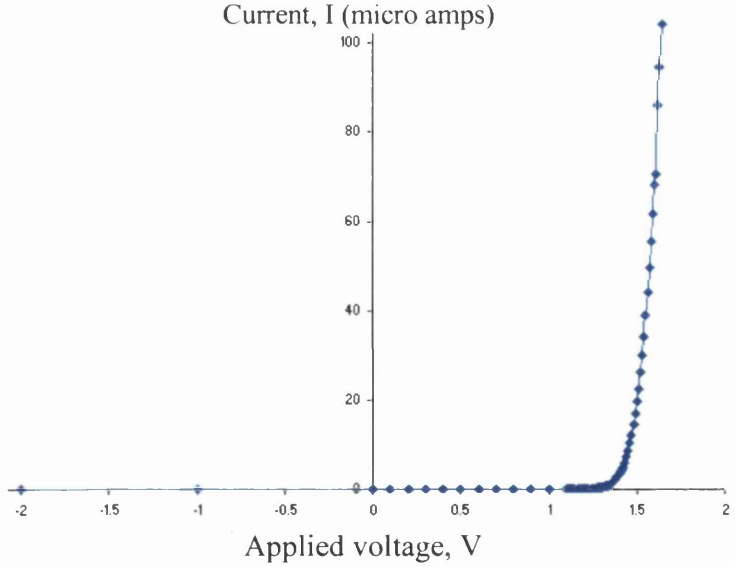

Figure 5.12: A typical I-V characteristic of Schottky diode obtained experimentally using the I-V technique.

This is a reasonable result showing the characteristics of a Schottky diode of nickel silicon carbide. The nickel was deposited using UHV evaporation system and the Ni layer thickness was about 50 nm. Further I-V measurements were made for all samples and dots that were tested by BEEM.

It is useful to plot the data using $\log_e$ of current versus the applied voltage in order to produce a linear plot of the data, as illustrated in figure 5.13.

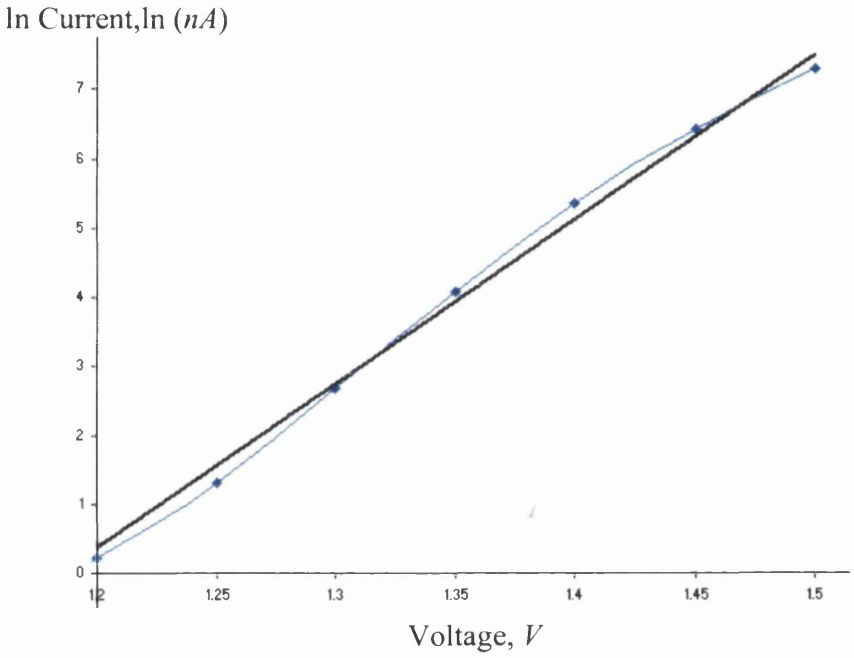

Figure 5.13: A $\log_e$ specific linear region I against V to show the forward characteristics.

The Schottky barrier can be calculated from the linear equation

$$y = 29.596\,x - 38.969$$

and using eq.(5.3) and eq.(5.4) and $T = 300K$, $A^* = 1.46\times10^6$, $e = 1.6\times10^{-19}$ and

$k_B = 1.38\times10^{-23}$

The Schottky barrier height is found to be $\phi_b = 1.57eV$ and the ideality factor is $n = 1.31$.

5.6 Final set-up

As discussed previously BEEM is a measurement technique requires a Schottky diode sample, an STM tip and amplifier circuits. Figure 5.14 shows the set-up that was finally used to produce the BEEM results. The setup seen below was used to investigate the Schottky sample behaviour and to study the barrier properties. Simultaneous STM and BEEM images were recorded at various tunnelling currents and bias voltages. Also, the Schottky barrier height was measured in different regions. In the following results chapter the system is tested and results from Ni contacts to SiC are presented.

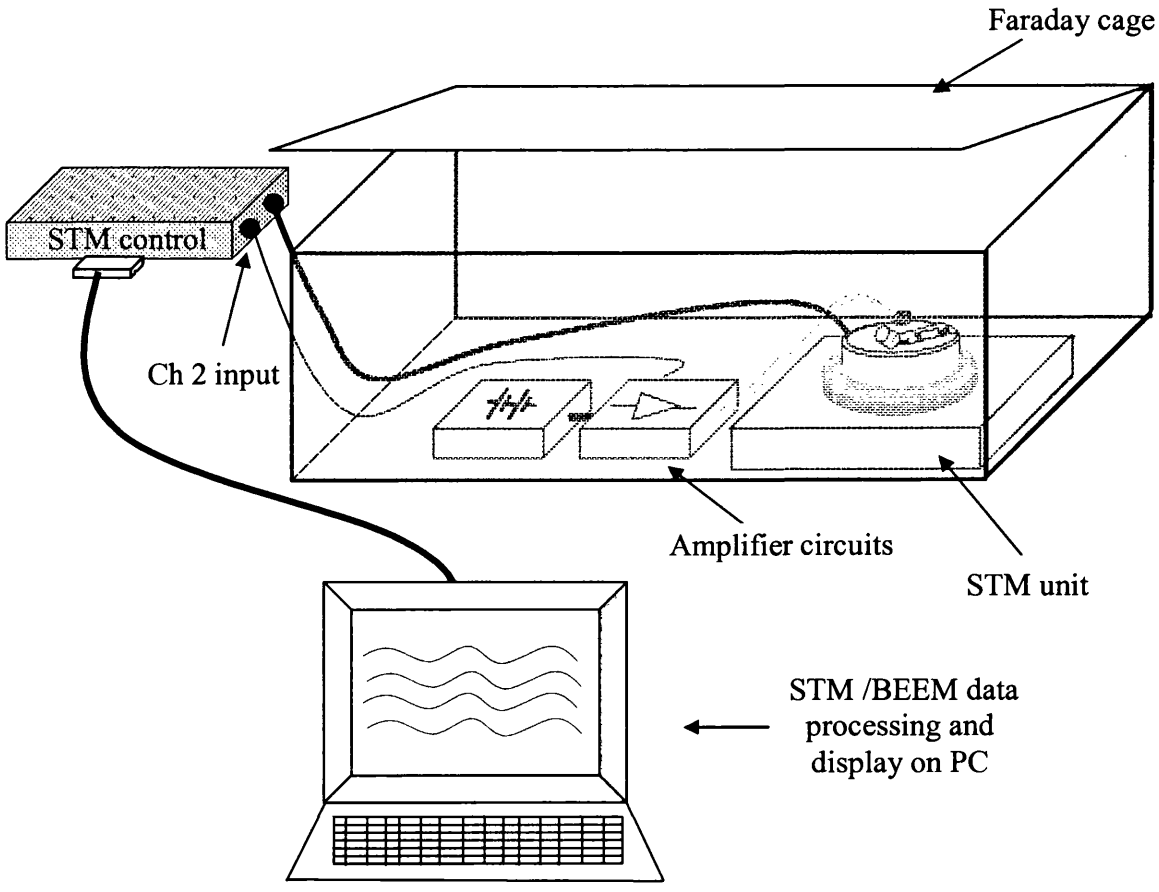

Figure 5.14: A typical experimental final set-up. The system is connected to amplifier circuits and STM control unit to Channel 2 input.

5.7 References

[1] Mathew Ackland, PhD thesis, University of Wales Swansea, (2005).

[2] Analogue Device, AD549- Product reference sheet.

[3] B. Pecz, Appl. Surf. Sci. **184**, 287 (2001).

[4] J.N. Su, A.J. Steckl, Inst. Phys. Conf. Ser. **142**, 697 (1996).

[5] M. Sochscki, J. Szmidt ,A. Werbowy, Jou. Of Wide band. Mat. **9** , 307, (2002).

Chapter 6

Results

6.1 Introduction

This chapter discusses scanning tunnelling microscopy (STM) and ballistic electron emission microscopy (BEEM) measurements taken on Ni-SiC contacts. The chapter addresses standard STM configurations and indicates the properties of the system once the third contact is made to the structure, (i.e. the earth contact made to the Ni overlayer). The chapter then addresses the formation of BEEM images and considers the surface properties of Ni-SiC Schottky contacts. Finally, quantitative measurements are made using BEEM spectroscopy (BEES) and are discussed in relation to macroscopic properties exhibited by the contacts.

6.2 Scanning tunnelling microscopy of Ni-SiC

STM can be used to examine Ni-SiC contacts and the probe local electronic transport properties on the nanometre scale. The implementation of a BEEM system requires an

understanding of the basic STM operation. To confirm the operation of the system, measurements were taken using the standard STM configuration to form a comparison. Figure 6.1 indicates the STM set up and basic energy band diagram. In the STM system is always grounded and a gap voltage is applied to the tip.

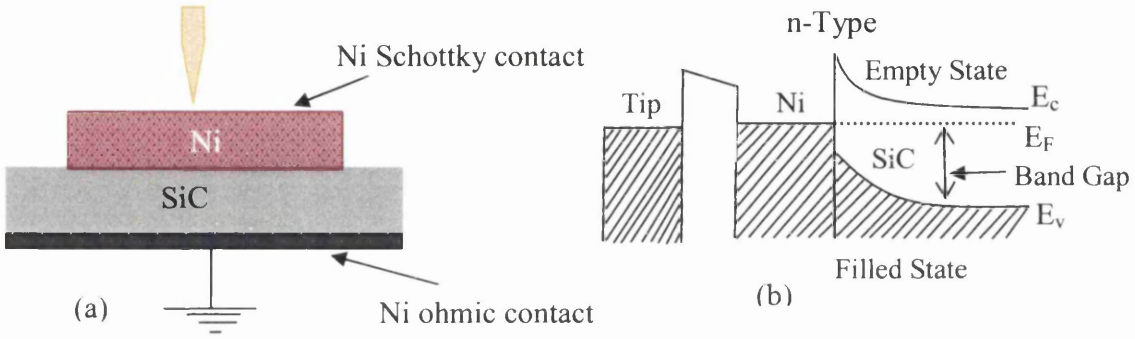

Figure 6.1: (a) Sample substrates with STM tip and (b) Energy band diagram.

When the tip was scanned over the thin metallic surface, a STM image of the metal overlayer was recorded as shown in figure 6.2(a). The image was made using the tip voltage of -1.58 *V* and tunnelling current of -1.92 *nA*. The image overleaf shows the metal clusters on the surface which vary in size and shape. These measurements were made towards the centre of the contacts. Variously sized Ni clusters were seen, the large clusters, were typically 40-50 *nm* in topographic height, whereas smaller clusters of height 20-30 *nm* can also be seen. These smaller clusters are become more prominent on smaller scale scans, as will be discussed later in section 6.3.

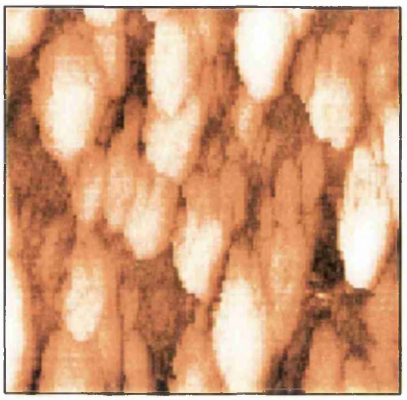

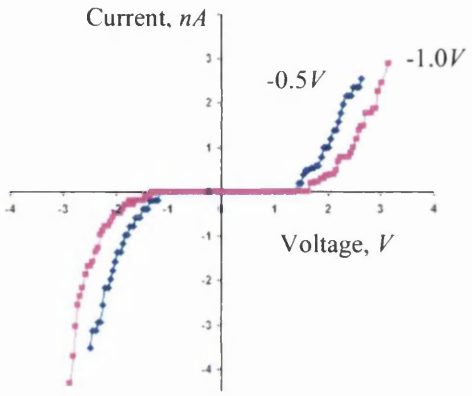

(a) (b)

Figure 6.2: (a) ($500 \times 500\ nm^2$) STM image of Ni deposited on SiC and (b) Typical I-V curves showing SiC band gap.

Furthermore, scanning tunnelling spectroscopy (STS) enables localised I-V curves to be recorded. As the sample is earthed via the ohmic back contact at the back of the SiC one would expect to see characteristics of the SiC manifested as a band gap. Figure 6.2(b) clearly shows a region of zero current. This was tested by changing the initial tunnelling conditions but still band gap properties can be seen (band gap is between 2.6 and 2.8 eV). However, due to the thickness of the metal these states and the on-set of current are complicated by localised microscopic and macroscopic properties of the surface and interface. To remove these surface factors an additional contact is required and BEEM measurements investigated.

6.3 STM & STS of metal contact with BEEM earth in place

The metal surface was then further examined using STM and STS, but three terminal connections were used instead of two terminals, as shown in figure 6.3. In this case the

majority of the tunnelling current will flow to earth via the third contact made to Ni overlayer, and the effective set-up for BEEM can be tested.

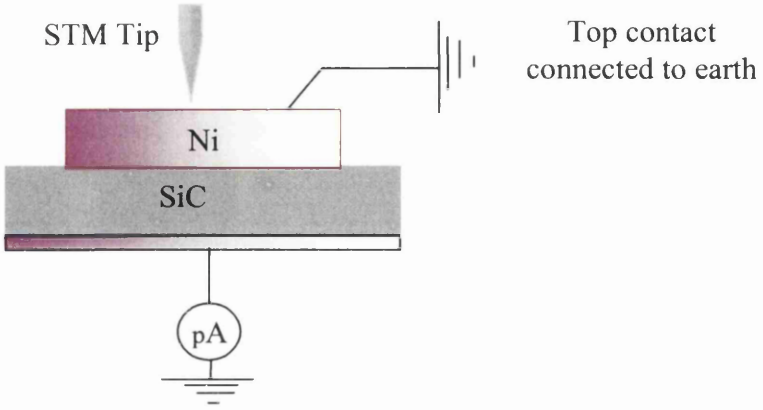

Figure 6.3: Two STM set-up terminals with a third BEEM connection.

As a result of this arrangement STM and STS measurements examine the structure and the electronic nature of the Ni surface. An STM image was recorded with negative bias voltage of -1.0 V and tunnelling current of $I_t = -0.9\ nA$, as shown in figure 6.4. This image was obtained on a small scale ($200 \times 200\ nm^2$) to study the cluster heights and to compare them with the image produced by the normal STM configuration system previously in section 6.2. The smaller image scale concentrates the attention on the smaller clusters that are present in the overlayer. The Ni cluster heights were measured from figure 6.4 and shown to vary up to 20 *nm*. The size of the clusters appears to change with Ni overlayer thickness and this is discussed in the following section 6.5.

In addition, the STS has been investigated with the same constant current but at different bias voltages of $V_T = -1.0\ V$ and $V_T = -0.5\ V$. This gives STS measurements at

different tip-sample distances. When looking at a conductor this is essential because the system always contains a tunnelling gap, and one would expect that the forward and reverse characteristic would appear very similar and that the tunnel gap (zero current region) would change with the tip-sample distance, indicating the conductive nature of the metal overlayer.

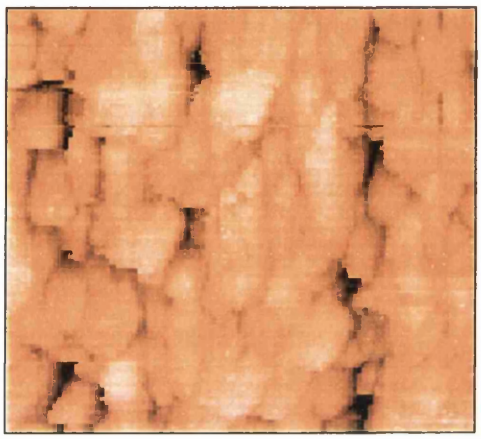

Figure 6.4: ($200 \times 200\ nm^2$) STM image with BEEM terminal connection on Ni.

Localised I-V curves were measured on clusters using a variety of different set-points (i.e. STM tunnel conditions). This then examined the effect of the tip sample distance. As can be seen in figure 6.5 the region of no current changes dramatically once the set-point voltage is changed from -1.0 *V* to -0.5 *V*. This confirms what we would expect for a conductor and indicates that the top contact is earthed and suitable for BEEM measurements. Note, the system is a fixed tip-sample distance when performing STS, thus the current sensitivity is dependent upon the initial set-point parameters.

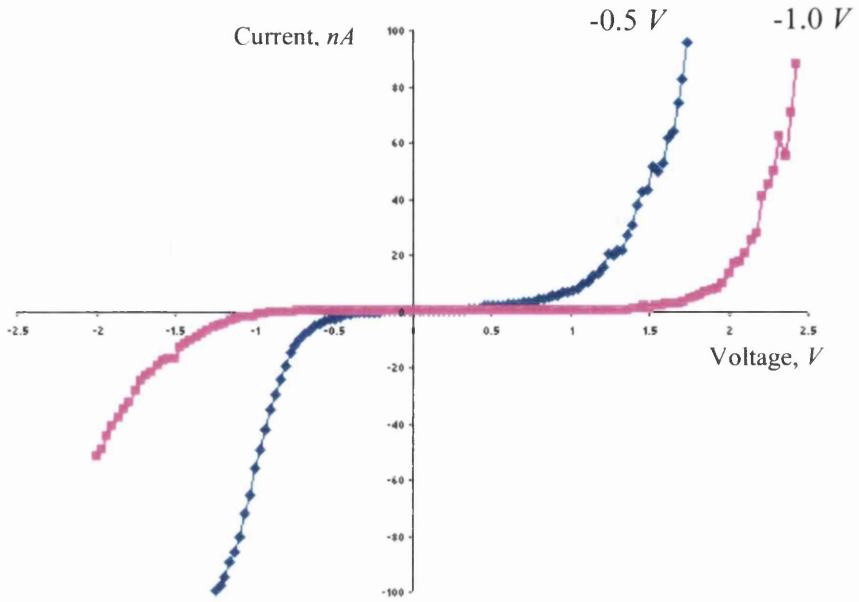

Figure 6.5: The I-V curves taking at different location on Ni's cluster.

As it has been mentioned previously, the tip-sample distance is fixed with the STS technique but it is very sensitive to the current set-point. The above results in figure 6.5 and the sensitivity of the tip-sample distance can be explained using a band diagram of tunnelling into a Schottky contacts.

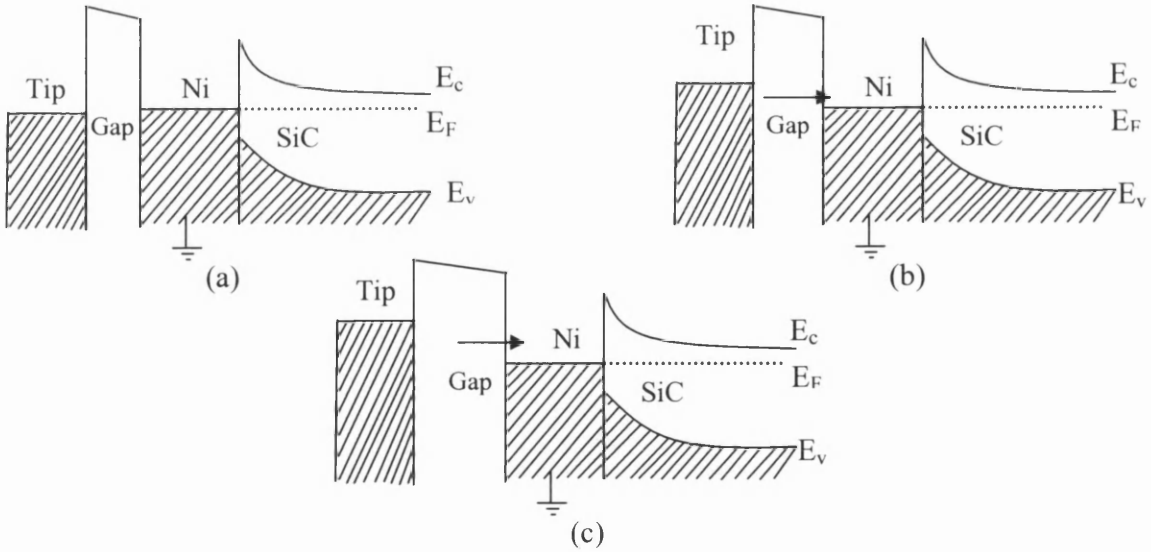

Fig 6.6: (a) Status of tunnelling at zero volts, (b) at -0.5 *V* and (c) at -1.0 *V* to maintain fixed tunnel current.

Figure 6.6(b) shows the gap to be smaller than in figure 6.6(c) due to the smaller gap voltage magnitude. Hence as it is closer to the STS measurements are more current sensitive.

6.4 Ballistic electron emission microscopy imaging

BEEM is a three terminal modification of the STM, and the previous section detailed how the STM system responds to an earth contact on the Ni overlayer. BEEM utilizes this earth contact and the full experimental set-up is shown in figure 6.7. This technique has the capability to obtain images of buried interfaces with nano-scale resolution[1] and it also enables the energy characterisation of such interfaces. Full theoretical considerations are discussed in chapter 4 and experimental issues are discussed in chapter 5.

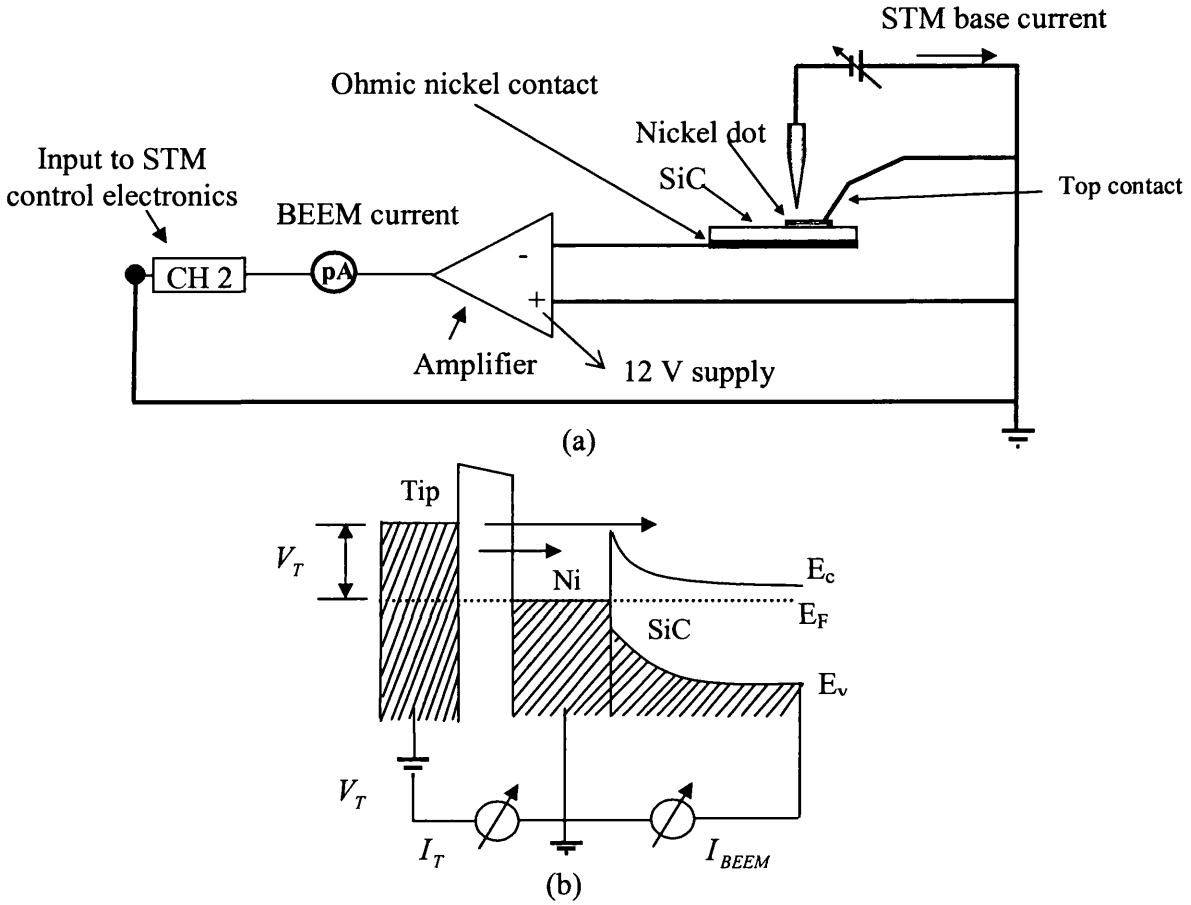

Figure 6.7: (a) Diagram of three terminals BEEM set-up and (b) Energy diagram of tunnelling.

6.5 Evidence of BEEM scans over the edge of the Ni

The scanning tip was placed on the edge of one of the nickel dots. Typically the dots are fabricated through a mask and the edge varies with thicknesses between 0.0 nm and 20 nm. Using a large negative bias voltage and choosing the edge of a Ni contact, maximized the ability of ballistic electrons to be measured and increased the probability to produce BEEM images. Figure 6.8 shows this in a schematic.

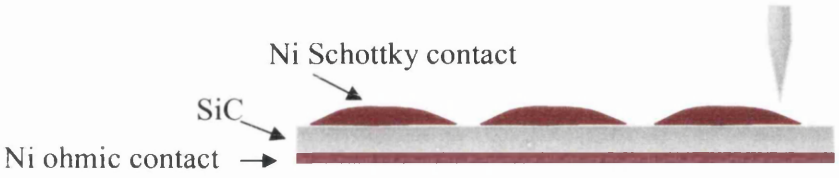

Figure 6.8: A cross section of Ni's dot deposited on SiC.

As can be seen in figure 6.9, the two images, the STM image and the channel 2 BEEM image clearly show the boundary of Ni and SiC on the edge of the contact. These images were obtained at a tunnelling current of -1 *nA* and a bias voltage of -3.5 *V*. Also presented are cross-section line profiles for comparison between the STM current and the collector current (BEEM current). The STM topography image shows the Ni clusters on the left hand side of figure 6.9(a) but, also a boundary and smoother SiC substrate on the right hand side. This is clearly seen in the corresponding BEEM image, as shown in figure 6.9(b). The separation is not uniform due to the nature of the mask and a dotted line guides the division. Also marked are horizontal lines to show the origin of the cross-section line profiles shown in figure 6.9(c) and figure 6.9(d). The simultaneous channel 2 BEEM current image is shown in figure 6.9(b), note that the right hand side of the image shows a much brighter contrast indicating a large current. Also note that due to the full range it is harder to see the

lesser detail of the BEEM image on the left hand side which will be discussed later in section 6.6. The line profile given in figure 6.9(d) gives further evidence of this greater current and in relation to figure 6.9(c) clearly showing saturation at the SiC region beyond the edge of the Ni. In this instance the tunnel conditions demand that over the bare SiC region the nano-ampere tunnel current is likely to flow to the back contact, hence saturating channel 2 and the pico amper amplifier. The edge measurements indicate that the BEEM system is working and that the measurements must now be focused on the detail of the Ni overlayer.

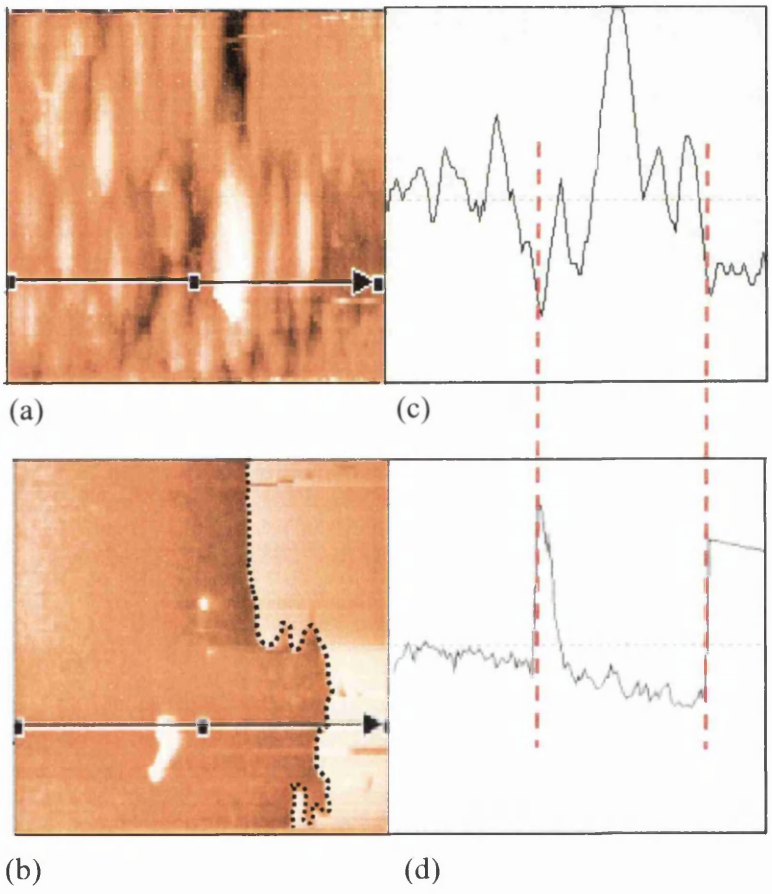

Figure 6.9: (a) shows an STM image of Ni contact and the edge onto SiC substrate ($272 \times 180\ nm^2$), (b) shows a corresponding channel 2 BEEM image, whilst (c) and(d) show their respective line cross-sections.

The BEEM current is highly sensitive to the overlayer thickness of Ni. It has clearly been shown from STM surface topographies that the cluster size of the surface can vary. It was found that the centre of the contacts showed cluster heights approaching 50 *nm* (see figure 6.2(a)) whilst closer to the dge of the contact cluster heights ~20 *nm* were seen (see figures 6.4 and 6.9(a)). It appears as thought the clusters coalesce together as the thickness increases. The varying thickness and non-abrupt nature of the edges is due to the mask deposition method, but this leads itself well to generate reproducible BEEM responsive regions. Care must be made as already shown when approaching the edge due to saturation of the amplifiers. Also damage near an edge can lead to isolated metal and again saturation of the BEEM channel 2.

Overall manufacture of contacts can be very time consuming until appropriate conditions are established. The following sections detail the more successful samples once conditions were optimised.

6.6 Large scale images

In order to obtain a BEEM sensitive region, a large scale image was used close to the contact edge, as seen in figure 6.10. The scan scale and metal thickness are $500 \times 500\ nm^2$ and $\sim 20\ nm$, respectively. The STM image figure 6.10(a) shows topography changes across the Ni overlayer and the dark region may be related to defect, such as surface scratches. The BEEM image figure 6.10 (b) reveal changes in BEEM current of ~ 5 pA and shows this region is BEEM active and suitable for study at higher resolutions.

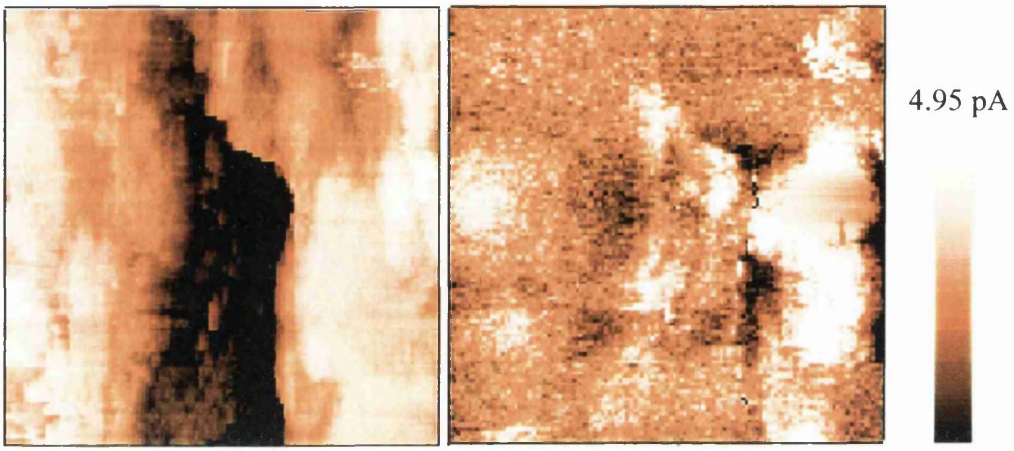

(a) (b)

Figure 6.10: ($500 \times 500\ nm^2$), (a) STM image and (b) BEEM image were recorded at tunnelling current of -1.0 *nA* and bias voltage of -1.7 *V*.

6.7 Small scale images

As already mentioned in the previous section, large scale images allow BEEM active regions to be revealed. Small scale images can be used to record a good BEEM image. Such an example is given a smaller scale image in figure 6.11(a) where the STM image shows some features of a number of metal clusters. The corresponding BEEM image in figure 6.11(b) shows bright and dark clusters which depend on areas of high and low ballistic current, respectively. The simultaneous STM and BEEM images were recorded at tunnelling current of -1.0 *nA* and bias voltage of -2.2 *V*. The STM image shows the structure of a Ni surface. As it can be seen uniform clusters are distributed on the surface of Ni (typically 15 – 20 *nm*). The BEEM image also shows the collector current and the edge effect of the clusters. The BEEM image shows different types of interface behaviour due to different barrier heights between Ni and SiC. There was some clustering present at both the surface and

interface when viewed as an image, but clear differences can be seen in the BEEM images of the contact.

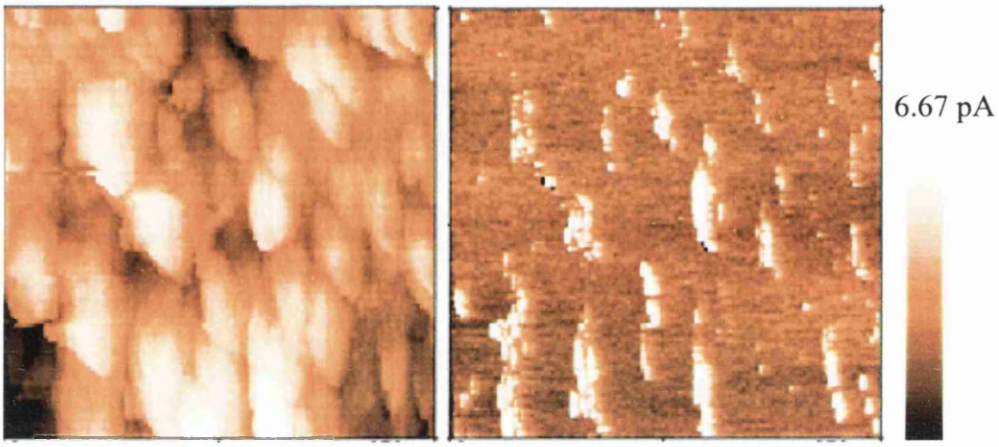

(a) (b)

Figure 6.11: (a) ($272 \times 272\ nm^2$) STM image and (b) BEEM image recorded at tunnelling current of -1.0 *nA* and bias voltage -2.2 *V*.

The possible scenario for BEEM response could be associated by the seeding of clusters growth by chemical reaction at the interface[2,3], which produces different barrier properties. This is discussed in more detail later in the conclusions when models for interface are discussed.

By further zooming in on such active regions greater resolution in the BEEM image is obtained, as shown in figure 6.12. The STM image, figure 6.12(a), again shows Ni clusters on the surface and these correspond well with previous Ni surface images near an edge with topographic heights between 3 nm and 10 nm. In this region BEEM were simultaneous acquired and more sensitive due to smaller cluster size. The BEEM image of figure 6.12(b) shows large variation (0-5 pA) and indicates an inhomogeneous interface with varying electrical properties.

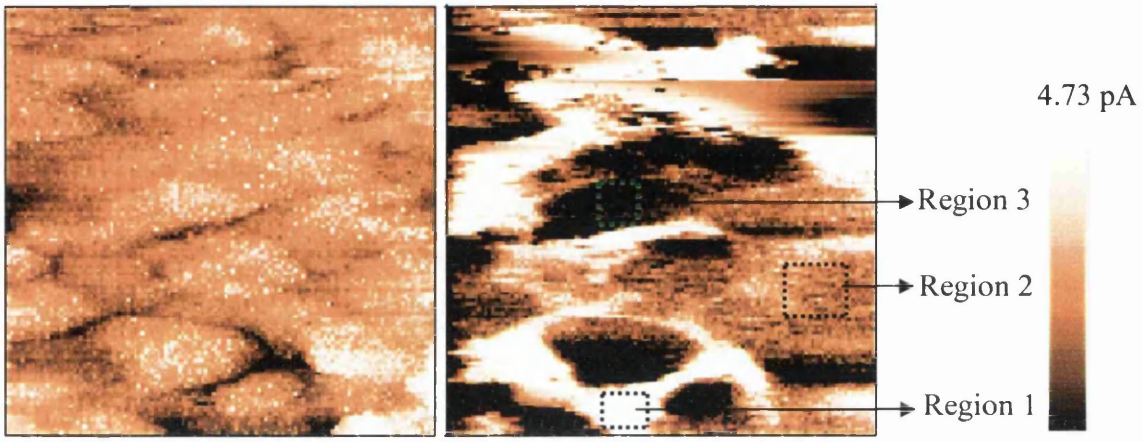

Figure 6.12: (a) ($188\times188nm^2$) simultaneous STM and (b) BEEM images recorded at a tunnelling current of -1.5 nA and a bias voltage of -2.5 *V*.

From this image BEEM currents appear to be greater in region surrounding clusters, and BEEM contrast can vary on clusters, going dramatically to zero on some regions. Region 1,2 and 3 are discussed in more depth via subsequent BEES measurements.

6.8 Ballistic electron emission spectroscopy (BEES)

BEEM can provide information on a variety of transport properties of ballistic electrons between Ni and SiC. However, BEEM images were also studied and observed by localised ballistic electron emission spectroscopy (BEES). Measurements were made to determine the Schottky barrier height values at different locations by observing the ballistic current as a function of voltage. Figure 6.13 shows the two BEEM spectra for Ni-SiC which were taken at different locations. Spectrum from figure 6.13(a) and spectrum from figure 6.13(b) were taken from dark clusters regions within the BEEM images, such as those in region 3 of figure 6.12(b), and show different values of threshold voltages 2.1 *V* and 2.35 *V*.

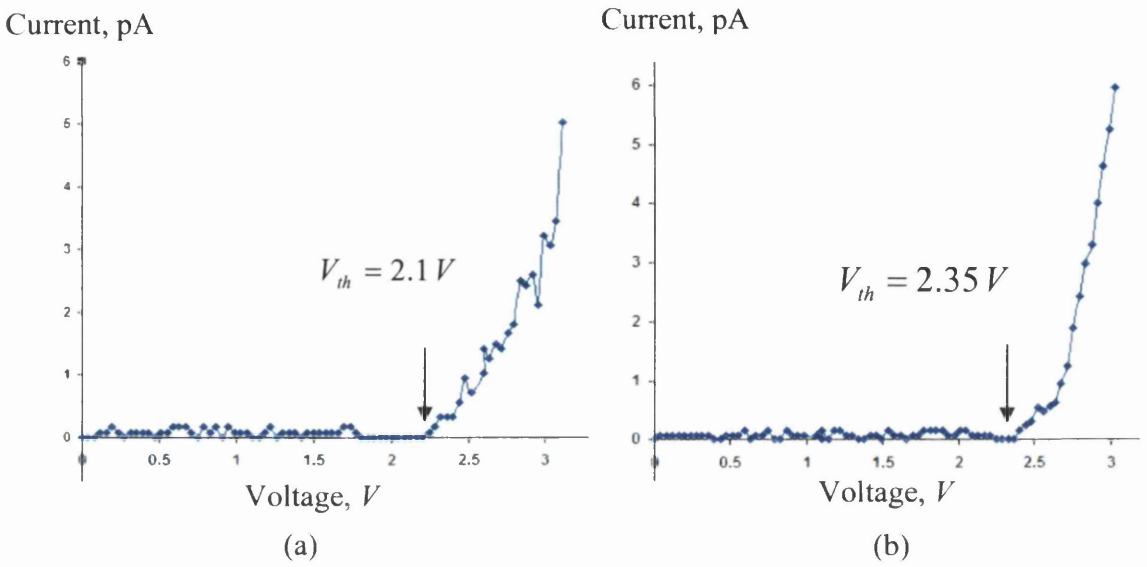

Figure 6.13: BEEM spectra taken at different low BEEM current locations.

Figure 6.14 also shows different values of threshold voltages when measured on regions with a very high current region 1 in figure 6.12(b) and average current regions, such as region 2 in figure 6.12(b). Threshold values of 1.48 V and 1.77 V were seen, respectively.

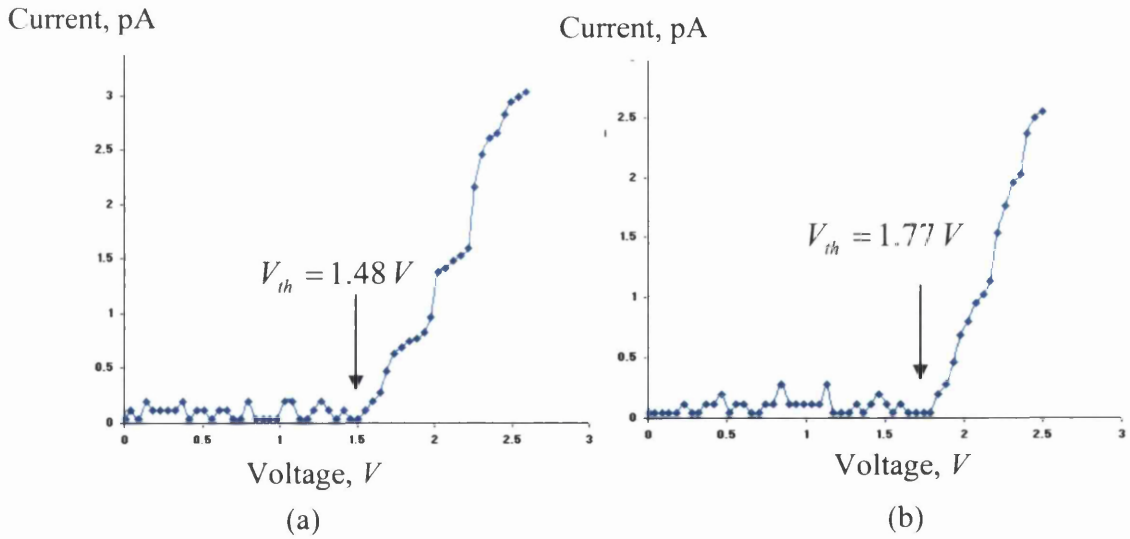

Figure 6.14: BEEM spectra taken at different high BEEM current locations.

6.9 Modelling the BEEM spectra and Schottky barrier height values

There are different methods are used to measure the Schottky barreir height, such as current-voltage (I-V) technique and etc., discussed earlier in chapter 2. This work employed BEEM with nano-scale resolution to investigate the possible variations of Schottky barrier height on the Ni-(4H)SiC system. In order to determine the exact values of Schottky barrier height, experiment data was fitted using the $(BK)^4$ model for BEEM spectra. The BEEM spectra exhibit a threshold voltage and thus represents the onset of a BEEM current. BEEM current can only be established once the Schottky barrier energy has been surpassed. By fitting with the BK^4 model (see chapter 4, equation 4.1) a theoretical fit was established to ensure the BEEM spectra matched the theoretical understanding[5]. Figure 6.15 shows the experiment data and its theoretical curve fit.

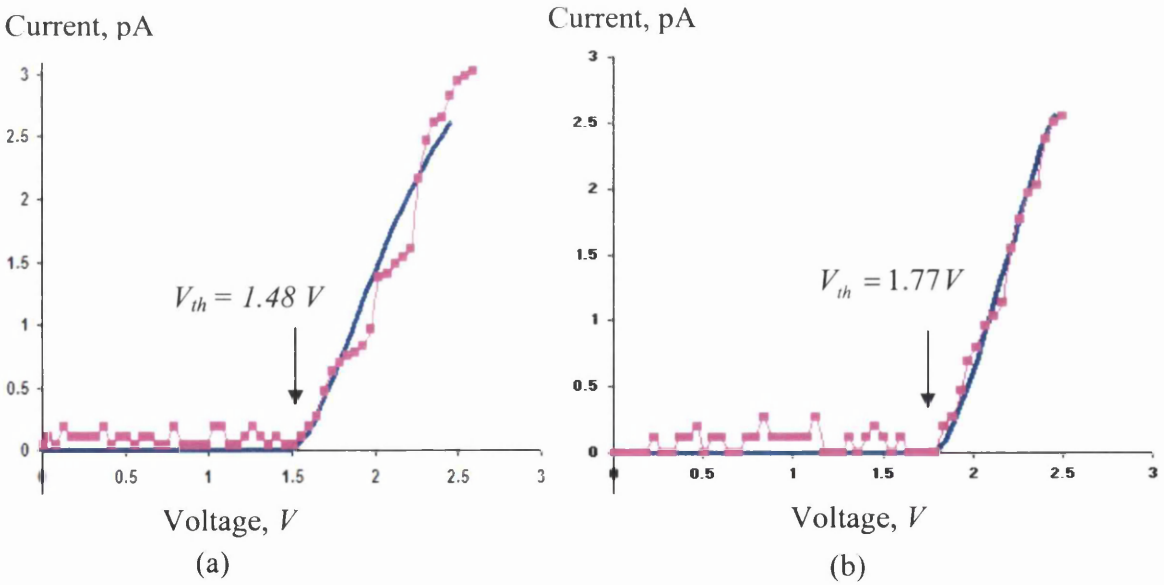

Figure 6.15: BEEM spectra for Ni on 4H-SiC taken at high BEEM current location (a) with tunnelling current of -1.3 *nA*, (b) with tunnelling current of -2 *nA*, and the line is a theoretical fit using equation 4.1. The value of threshold voltage is shown above the BEEM spectra .

The values of Schottky barriers used in the fits were 1.48 *V* and 1.77 *V*, but more importantly the data supports the overall BK model. This type of theoretical fit was applied to all BEEM spectra and the values correspond to a varying Schottky barrier heights between Ni and SiC. Overall, threshold results and Schottky values coincided and were seen to vary between 1.48 *V* and 2.35 *V*. Macroscopic I / V measurements indicate that the Schottky barrier height is typically 1.57 *eV* for these diodes, but their idealities can be greater than 1.3. The variation in the BEES threshold measurements indicates the inhomogeneous nature in the contact properties and the likely origins of the poor ideality[6,7]. In the conclusions chapter the nature of the contact between Ni-SiC is discussed in terms of these results, and others reported in literature.

6.10 References

[1] W. J. Kaiser, M. H. Hecht, R. W. Fathauer and L. B. Bell, Phys. Rev. B, **44**,6546 (1991).

[2] A. Fernandez, H. D. Hallen, T. Huang, R. A. Buhrman, and J. Silcox, appl. Phys. Lett., **57**,2826 (1990).

[3] G. John, PhD thesis, University of Wales Swansea,2004.

[4] L.D. Bell and W.J. Kaiser, Phys. Rev. Lett. **61**, 2368 (1988).

[5] H.-J. Im, B. Kaczer, J.P. Pelz, W.J. Choyke, Appl. Phys. Lett. **72**,839 (1998).

[6] A. Fernanez, H. D. Hallen, T. Huang, R. A. Buhrman, and J. Silcox, Appl. Phys. Lett., **57**, 2826 (1990).

[7] F. Roccaforte, F. La Via, V Raineri, R. Pierobon, and E. Zanoni, Mater. Sci. Forum, **457**, 869 (2004).

Chapter 7

Conclusions

7.1 Summary

Developments made to a standard desktop, in air, STM via a 3rd contact and pA current amplifiers have been successful in allowing BEEM measurements to be made on the interface properties of Ni-SiC contacts. It has been proven that such a BEEM system conforms well to expected tests and that pA currents can be observed with noise level less than 1 pA. Moreover, simultaneous STM and BEEM imaging is possible and spectroscopic BEEM data attainable. Studies on Ni-SiC produced STM images which showed that the Ni surface is clustered and these clusters can vary in height depending on overlayer thickness. As a result of the preparation process, the BEEM experiments were focused on the edge of the Ni fabricated dot because this area proved a very active region for ballistic current formation due to the smaller cluster heights (~10 *nm*). Since each sample could be processed into approximately 25 diodes, the measurements were based upon active diodes in order to obtain reproducible results. BEEM images showed varying current response and contrasts indicating a variation in the electronic nature of the intrface which required further analysis

via more detailed BEES measurements. Threshold voltages obtained from the BEEM spectra indicated significant differences across the interface infering that the Schottky barrier varied in those regions. Several groups[1,2,3] have used BEEM and BEES to study Schottky barrier heights in a similar fashion.

Moreover, Schottky barrier heights can be determined from the (BK) model[3,4] by applying the theoretical model to the BEEM spectra, and this proved successful in this work. The threshold results and I_c/V characteristics matched well with theoretical fits, made with defined Schottky barrier heights, and values were seen to vary between1.48 e*V* and 2.35 e*V*. The standard I-V measurements indicated that the Schottky barrier height is typically 1.57 *eV* for these diodes, but their ideality factors are normally greater than 1.3. These values further support the large variations of Schottky barrier measured and indicates the inhomogeneous nature of the room temperature deposited Ni-SiC interface, as seen in the BEEM images[5].

7.2 A proposed Ni-SiC model

It has previously been reported that the Schottky barrier height value changes[6,7] when Ni-SiC samples are annealed and studies have considered temperatures ranging from room temperature to more than 1000^0C. When deposited at room temperature, a 20 Å Ni contact has been shown to exhibit a Schottky barrier of 1.31 *eV* and when the temperature is increased to 600^0C, the Schottky barrier increases[7] to 1.72 *eV*. However, the Schottky contact changes to an Ohmic contact at high temperature annealing, such as 900^0C and 1000^0C[7,8]. After annealing at a high temperature, it has been proposed that a reaction layer forms at the interface and the model for ohmic nature is based upon defects and production of voids[9]. It is clear that annealing processes can produce chemical changes and surface defects[7,9].

In our studies, BEEM was used to study Ni-(4H)SiC at room temperature and highlighted regions of Ni clusters of with Schottky barriers varying in height from 1.77 *eV* to 2.35 *eV*. Moreover, regions between clusters (inter-cluster regions) with barrier 1.48 *eV* were also seen. It is known that even with room temperature deposition and Schottky formation, a limited chemical reaction occurs between Ni and SiC (Secondary ions mass spectrometry (SIM) and Resonant ionization mass spectrometry (RIMS) measurements of G. John[10]), but the interface is relatively abrupt. However, Ni-Si bond formation is promoted by annealing to 500^0C[6,7] and Schottky barrier heights increase. Indeed, G. John[10] showed that annealing such samples increased Ni cluster size, as the clusters aggregate together and form a more continuous overlayer. Reactions between Ni and Si are more likely to have occurred beneath a cluster and results here show that these regions have a higher barrier. As annealing results have shown (G. John[10]) clusters get bigger and (the lower barrier) inter-cluster regions decrease. The net effect is a more homogeneous contact with higher barrier regions produced. It appears that reactions between Ni and SiC at room temperature might well generate the dynamics for the cluster formation which would then be increased by annealing to 500^0C.

7.3 Future work

The vital goal of this work was achieved and showed the success of studying the properties of Ni-SiC contacts with the developed BEEM system. However, there are several ways the investigation of metal contacts to SiC can be improved and expanded. For example studying the effects of annealing on the localised Schottky barrier height would further enhance understanding of this system, it has been shown that electrical properties and topographical information, such as chemical reaction and defects can be studied using BEEM

and BEES techniques and there exists an opportunity to examine alternative surface preparation and metal overlayers. In addition, other diode based samples can be investigated using the design of the system presented here, such as laser diodes.

Developing BEEM on a UHV system would obviously benefit the acquisition in terms of noise and sample stability. Finally, using a STM with a translating sample would be for more productive and alleviate many of the difficulties in using the desktop STM/BEEM system.

7.4 References

[1] W. J. Kaiser, M. H. Hecht, R. W. Fathauer and L. B. Bell, Phys. Rev. B, **44**,6546 (1991).

[2] M. Rubin, H. Blank, M. Chin, H. Kroemer and V. Narayanamurti, Appl. Phys. Lett.,70,1590(1997).

[3] H.-J. Im, B. Kaczer, J.P. Pelz, W.J. Choyke, Appl. Phys. Lett. **72**,839 (1998).

[4] B. Kaczer, H.-J. Im, J.P. Pelz, J. Chen, W.J. Choyke, Phys. Rev. B **57** , 4027 (1998).

[5] H. von Kanel and T. Meyer , Thin Solid Films, **306** , 214 (1997).

[6] A. Kestle. S. P. Wilks, P. R. Dunstan, M. Pritchard and P.A. Mawby, Elect. Lett. Vol.**36**, 267 (2000).

[7] W.Y. Lee, PhD thesis, Chapter 7, University of Wales Swansea,2004.

[8] O. J. Guy , G. Pope, I. Blackwood, K.S. Teng, L. Chen. W.Y. Lee, S. P. Wilks, P.A. Mawby, Surf. Sci. ,**573**, 253, (2004).

[9] F. Roccaforte, F. La Via, V Raineri, R. Pierobon, and E. Zanoni, Mater. Sci. Forum, 457, 869 (2004).

[10] G. John, PhD thesis, University of Wales Swansea,2004.

Appendix A: Calibration Sheet for STM Unit

Previous calibration values1		**Previous** calibration values 2		**New** calibration values	
Scan Axis0	400 nm	Scan Axis0	501 nm	Scan Axis0	477 nm
Scan Axis1	250 nm	Scan Axis1	313 nm	Scan Axis1	323 nm
Scan Axis2	100 nm	Scan Axis2	100 nm	Scan Axis2	100 nm
Channel0	100 nA	Channel0	100 nA	Channel0	100 nA
Channel1	100 nm	Channel1	100 nm	Channel1	100 nm

This is a grid sample ($160\,nm^2$) in the STM unit

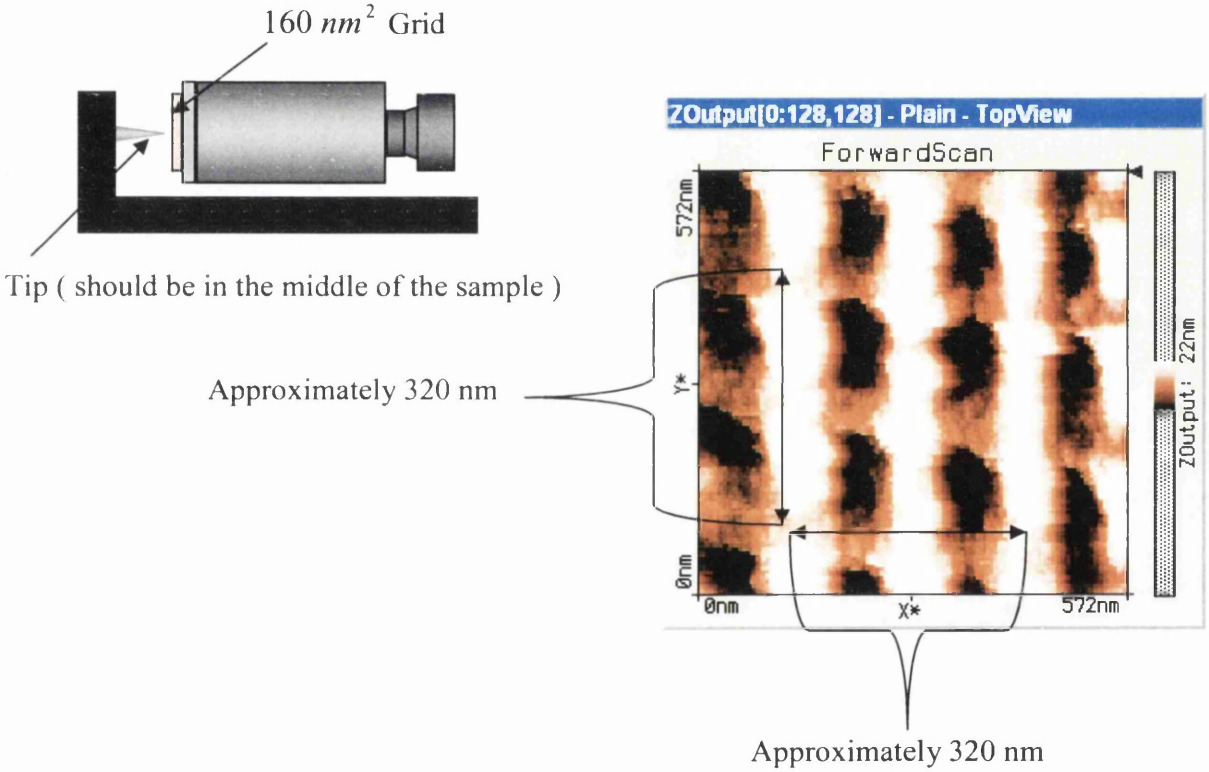

These are the settings for above topography

Date 24-03-2004 Time = 17:01:35

Scan Range	= 572 nm	X slope	= 0^0	Gap Voltage	= 0.5 V
Z Range	= 200 nm	Y slope	= 0^0	Set Point	= 1 nA
Time / line	= 0.255 s	X Offset	= 0nm	P gain	= 13
Input Range	= 12.5 nA	YO ffset	= 0nm	I gain	= 12
Rotation	= -4^0	ZO ffset	= 0nm	Loop Mood	= Run
Scan Dir	= Up			Scan Head	= STM

Appendix B: Ex-situ SiC wafer cleaning techniques

The following procedures are used to clean SiC wafers prior to deposition of Ni electrical contacts for both the high vacuum Edwards evaporator and ultra-high vacuum deposition techniques. The process removes dust, oil based contaminants, organic substances, ionic contaminants, and etches SiO_2 surface oxides without modifying SiC, leaving an atomically clean surface

A - Solvent Clean

1- Trichloroethylene (15 minutes)

2- Acetone (15 minutes)

3 – Iso- propanal (15 minutes)

4 – Methanol (15 minutes)

B - Pirana Clean

1- 5 ml H2 SO_4 (Sulphuric Acid) + 1 ml H2 O_2 (Hydrogen Peroxide)

2 - After 5 minutes : 1 ml of H_2 O_2

3 - After 5 minutes : 1 ml of H_2 O_2

C - RCA Clean

1- 1 ml NH_4 OH (Ammonia or Ammonia Hydroxide) + 5 ml H_2 O + 1 ml H_2O_2

at 75 degrees Celsius (15 minutes)

2 – HF dip (30 secs – 2 minutes)

3 – 1 ml HCl (Hydrochloric Acid) + 5 ml H_2 O + 1 ml H_2O_2

at 75 degrees Celsius (15 minutes)

4 - HF dip (30 secs – 2 minutes)

Rinse between steps with H_2 O